Canadian Journal of Physics

Research Article

Spectra of phosphorus ions for astrophysical modeling: P I–P XV

Sultana N. Nahar[a] **and Bilal Shafique**[b]

[a]Department of Astronomy, The Ohio State University, Columbus, OH 43210, USA; [b]Astronomy, The Ohio State University, Columbus, OH 43210, USA

Corresponding author: **Sultana N. Nahar** (email: nahar.1@osu.edu)

Abstract

Phosphorus (P), a basic element of life, has been a least studied element due to its poor presence in astrophysical spectra. However, search for the P lines has increased considerably with discoveries of exoplanets and are being detected by high resolution and sophisticated astronomical observatories, e.g., James Webb Space Telescope (JWST). JWST may provide a clue for life with detection of P in its infrared (IR) region. Identification of the element and analysis of the observed spectra will require high accuracy data for atomic processes that produces lines and their predicted features. The present study focuses on these needs and reports systematically regions of wavelengths, from X-ray to IR, that show prominent lines by the 15 individual ionization stages of phosphorus, P I–P XV for the first time. We present large amount of relevant atomic data for energies, transition parameters, and lifetimes obtained in relativistic Breit–Pauli approximation using the R-matrix method and atomic structure program SUPERSTRUCTURE. Our spectral features for the 15 ions, P I–P XV, predict strengths of lines in various wavelength regions. They show dominance of P I and P II in the IR region and other ions in the ultraviolet and optical regions often stretching to IR in the continuum. For determination of accuracy, we have made extensive comparisons of our atomic data with available experimental and theoretical values. Based on these, our results and features are expected to provide precise plasma diagnostics and astrophysical modeling.

Key words: phosphorus ions, oscillator strengths, lifetimes, spectral features, photo-excitation cross sections

1. Introduction

Chemical elements, such as, carbon, nitrogen, oxygen, phosphorus, sulfur form the basis of human life on the Earth. Phosphorus (P) is contained in DNA–RNA and acts as an energy carrier, and hence plays a key role as a biosignature element. It is abundant in the solar system but lacks in space. The lack of P is often linked to not finding any life form outside the Earth. Hence, with discoveries of exoplanets, phosphorus is holding a special importance to astrobiology as its relative abundance in a planetary host star will increase the prospects for life on its planet [1]. Search of its lines in the exoplanetary atmosphere has increased considerably. James Webb Space Telescope (JWST) is expected to obtain high-resolution spectra in the infrared (IR) region of 0.6–28.3 μm which includes a few ionization stages of phosphorus. Phosphorus has been detected in a number of astronomical objects, such as, in damp Galaxies [2, 3], in nebular environments of supernova remnants of Cassiopeia [4]. Lines of P II and P III have been found in the high resolution spectra of hot OB stars under a project called ASTRO-2 (J. Hillier, private communication 2015). However, poor abundance caused limited number of investigations of the element and hence a limited amount of atomic data available for spectral analysis of various ionization stages of P.

Existing data of P ions are largely for energies for all ionization stages from P I to P XIV measured by Martin et al. [5] and for P XV measured by Yerokhin and Shabaev [6], and Erickson [7]. These energies are available in the compiled tables at the website of National Institute of Standards and Technology (NIST) [8]. Literature search shows that the other atomic data available are mainly for radiative transitions in a limited manner and radiative lifetimes of levels measured using beam-foil, fluorescence detection technique, and in storage ring and cyclotron experimental setups. Only a few studies have been done for other atomic processes, such as, photoionization, electron–ion recombination, electron impact excitation, for astrophysical plasma modeling applications. A brief summary of the past studies on the atomic processes for each P ion is given below.

1.1. P I

NIST [8] compiled table reports transition probabilities calculated by Lawrence [9], Czyzak and Krueger [10]. Energies for fine structure levels, radiative decay rates for both allowed (E1) and forbidden (M1, E2, M2, and E3) transitions, and life-

times for a number of levels of neutral phosphorus (P I) along with other ions in isoelectronic sequences from sodium (Na) through Argon (Ar) were calculated by Zatsarinny and Frose-Fischer [11] and Frose-Fischer [12]. Lifetimes for the 21 excited states of phosphorus ions (P I through P V) were measured by Curtis et al. [13] from the spectra of phosphorus in the UV region (600–2200) Å using beam–foil technique. Berzinish et al. [14] measured lifetimes of P I using fluorescence detection method.

1.2. P II

Transitions in P II were studied by several investigators [10, 15–17]. The calculations for P II transitions were carried out using the MCDF atomic code developed and revised by Desclaux [18]. Later Huang [19], Brown et al. [20] reported calculated energies and transition probabilities of P II. Curtis et al. [13] and Brown et al. [20] measured lifetimes of P II. Photoionization cross sections of many excited levels going up to $n = 10$ of P II were obtained using relativistic Breit–Pauli R-matrix (BPRM) method by Nahar [21]. Photoionization cross sections of the ground and low lying excited levels of P II were benchmarked with experiment carried out at the Advanced Light Source at LBNL by Nahar et al. [22]. Nahar [23] studied electron–ion recombination of P II using the unified method of Nahar and Pradhan [24, 25]. All atomic data for photoionization and electron–ion recombination are available electronically at the NORAD-Atomic-Data database [26].

1.3. P III

The transitions in P III were studied by Wiese et al. [17], Fuhr et al. [15], Huang [27], Naqvi [28]. Naqvi calculated a single M1 forbidden transition. Huang [27] reported energies and transition probabilities of P III along with other Si-like ions. Measurement of lifetimes of phosphorus ions by Curtis et al. [13] included those of P III. Measured spectra of photoionization cross sections for P III and P IV for the ground and a few low lying levels were reported by Hernándeza et al. [29] and the measured resonances were identified theoretically by Gning et al. [30]. The electron impact excitation collision strength and rates for P III obtained using BPRM method by Naghma et al. [31].

1.4. P IV

Transitions in P IV were studied by Zare [32], Crossly and Dalgarno [33]. Naqvi [28] calculated M1 transitions among the levels of $3sp3(^{1,\,3}P^{o})$. Lin et al. [34] used the semi-empirical model potential method to calculate the excitation energies and magnetic quadrupole (M2) transition rates for Na-, Be-, and Mg-like ions (including P-IV). Godefroid et al. [35] measured and calculated the relative intensities of the E2 transitions of P IV and P V. Measured lifetimes of various levels of phosphorus ions have been reported by Curtis et al. [13] which included those of P IV, Brown [20], Alkhayat [36], Van Der Westhuizen et al. [37], Maio [38]. Photoionization cross sections for P IV were measured by Hermandeza et al [29] and resonances calculated by Gning et al. [30].

1.5. P V

Transitions in P V were studied by several investigators [17, 33, 35, 39]. Godefroid et al. [35] measured and calculated the relative intensities of the E2 transitions of P IV and P V. Lifetimes of P V were measured by Curtis et al. [13] and Maio [38].

1.6. P VI

Earlier calculations for a limited transitions in P IV were carried out by Kastner et al. [40]. Hibbert [41] reported a large set of atomic data for level energies, oscillator strengths, lifetimes for neon-like ions (Ne-I through Kr XXVII) which included P VI using the general-configuration interaction code, CIV3, which incorporates the optimized orbitals and a modified Breit–Pauli approximation. Zhu et al. [42] used GRASPVU atomic code package, a modified version of the general-purpose relativistic atomic structure package GRASP92, and computed transition wavelengths, transition probabilities, line strengths and the oscillator strengths for nine charged states of phosphorus (P VI through P XIV).

1.7. P VII

The earlier work on the radiative transitions in P VII include those of Cohen and Dalgarno [43], Naqvi [28], Aggarwal [44]. Aggarwal reported theoretical calculations of level energies for 198 levels, transition probabilities, and radiative lifetimes for F-like ions ($12 \leq Z \leq 23$) which included P VII. He used Flexible Atomic Code which uses the relativistic approached based on Dirac equation for level energies and the GRASP to calculate the radiative transition rates and lifetimes for the electric dipole and quadrupole transitions (E1 and E2) and the magnetic dipole and quadrupole transitions (M1 and M2). Cheng et al. [45] reported transition probabilities for electric dipole (E1), quadrupole (E2), and magnetic dipole transitions for Li through F ioselectronic sequences of various ions including P VII through P XIV using MCDF method. Zhu et al.'s [42] calculations included the energies and transition parameters for P VII.

1.8. P VIII

Transitions in P VIII have been studied by Cohen and Dalgarno [43], Cheng et al. [45], Naqvi [45], Malville and Berger [46], Zhu et al. [42]. Träbert et al. [47] used test storage ring (TSR) set-up to measure lifetimes of $2s^2 2p^2\ {}^1D_2$, $2s^2 2p^3\ {}^2P^{o}_{1/2,3/2}$, and $2s^2 2p^4\ {}^1D_2$ levels of various ions (Si through S) including P VIII, P IX, and P X.

1.9. P IX

Transitions for P IX have been studied by Cheng et al. [45], Zhu et al. [42], Cohen and Dalgarno [43], Naqvi [45]. Träbert et al. [47] used TSR set-up to measure lifetimes of levels of P IX.

1.10. P X

Energies and transition parameters for P IX were calculated by Cheng et al. [45], Zhu et al. [42], Cohen and Dalgarno [43], Malville and Berger [46], Froese-Fischer [48], Naqvi [28] reported energies and transition parameters for P X. Träbert et al. [47] reported lifetimes of levels of P X.

1.11. P XI

Cheng et al. [45], Zhu et al. [42] reported energies and transitions in P XI. Cohen and Dalgarno [43], Naqvi [28], Wiese et al. [17] also reported study of transitions in P XI.

1.12. P XII

Energies and transitions of P XII were reported by Cheng et al. [45], Zhu et al. [42], Naqvi [28], Garstrang and Shamey [49], Cohen and Dalgarno [43], and Naqvi and Victor [50]. From the analysis of decay curves obtained from Beam–Foil excitation Träbert and Heckmann [51, 52] deduced the lifetimes in the EUV region (10 Å- 550 Å) for P XI.

1.13. P XIII

Transitions have been calculated by investigators [17, 42, 43, 45]. Experimental radiative decay rates of transitions in Li- and He-like P-ions have been reported by Deschepper et al. [53] using Doppler-tuned X-ray spectrometer for the acquisition of highly resolved spectra in X-ray region.

1.14. P XIV

Cheng et al. [45], Zhu et al. [42] reported the energies and transition parameters for P XIV. As mentioned above, measured radiative decay rates of transitions of He-like P-ions have been reported by Deschepper et al. [53], Wiese et al. [17], Cohen and Dalgarno [43], Drake [54], and Lin et al. [55].

1.15. P XV

The one-photon transition probabilities for H-like ions with nuclear charges $1 \leq Z \leq 100$ (including P XV) using the relativistic quantum theory were reported by Popov and Maiorova [56].

The objectives of the present work is to obtain large set of energy levels and the transitions among them, and implement them to study and predict the domain of prominent spectral features in broad wavelength ranges, from X-ray to IR, for all 15 ionization stages of phosphorus, P I–P XV. The present study is the first systematic study for a relatively complete spectral features of all ionization stages of phosphorus. Detection of features can lead to determination of presence of the element in astronomical objects and identify the ionization stages for modeling. We have considered transitions from orbital 1*s* to going up highly excited states. There are other atomic processes in addtion to photo-excitation that contribute to the formation of a spectrum. For example, photoionization enhances the background and strengthens the peaks of the spectral lines and may even appear as absorption lines in the continuum. Electron–ion recombination and electron-impact excitation also introduce lines that are used for diagnostics of the plasma. But a spectrum and its features are mainly created by photo-excitation.

We have employed the relativistic BPRM method as adopted under the Opacity Project [57] and the Iron Project [58] as well as atomic structure calculations in Breit–Pauli approximation as adopted in program SUPERSTRUCTURE (SS) [59, 60] to calculate oscillator strengths and other transition parameters for photo-excitation and create the absorption spectra. We present in the next section a brief outline of the theoretical backgrounds that were used to obtain the photo-absorption spectra of phosphorus ions.

In the present study, we report photo-absorption features along with atomic data for bound state energies, radiative transition rates and lifetimes of all phosphorus ions, P I through P XV. For accuracy estimation we have compared the present atomic data with those available in literatures. All atomic data of the present work will be available electronically at NORAD-Atomic-Data database [26].

2. Theory

Discrete lines are formed from atomic photo-excitation. The process of photo-excitation of ion X^{+Z}, where X is the ion of charge Z, may be expressed as

$$X^{+Z} + h\nu \rightleftharpoons X^{+Z*} \tag{1}$$

where $h\nu$ is the photon and * indicates an excited state. The process can also lead to a doubly excited state. The absorption spectral features for all 15 ionization stages of phosphorus in the present work were generated using oscillator strengths of large number of photo-excitation for each ion.

Two methodologies are employed here, relativistic BPRM method [57, 58] for P I and P II, and atomic structure calculations using program SS in Breit–Pauli approximations [59, 60] for all P ions, P I–P XV. While BPRM can generate a much larger set of dipole allowed E1 transitions, SS can compute both dipole allowed E1 and forbidden electric quadrupole (E2), electric octupole (E3), magnetic dipole (M1), magnetic quadrupole (M2) transitions. Calculations using BPRM codes [61, 62] are ab initio that do not use any model potential, SS [59, 60] implements Thomas–Fermi–Dirac–Amaldi potential to represent the electron–electron interactions.

In relativistic Breit–Pauli approximation, the Hamiltonian in Schrodinger equation

$$H_{\rm BP}\Psi = E\Psi \tag{2}$$

is given by (e.g., [60, 63])

$$H_{\rm BP} = H^{\rm NR}_{N+1} + H_{\rm mass} + H_{\rm Dar} + H_{\rm so} + \frac{1}{2}\sum_{i\neq j}^{N}\left[g_{ij}\left(so + so'\right) + g_{ij}\left(ss'\right) + g_{ij}\left(css'\right) + g_{ij}\left(d\right) + g_{ij}\left(oo'\right)\right] \tag{3}$$

where $H^{\rm NR}_{N+1}$ is the non-relativistic Hamiltonian

$$H^{\rm NR}_{N+1} = \sum_{i=1}^{N+1}\left\{-\nabla_i^2 - \frac{2Z}{r_i} + \sum_{j>i}^{N+1}\frac{2}{r_{ij}}\right\} \tag{4}$$

The next three terms are 1-body correction terms known as the mass correction, Darwin and spin–orbit interaction

terms,

$$H^{\rm mass} = -\frac{\alpha^2}{4}\sum_i p_i^4 \qquad H^{\rm Dar} = \frac{\alpha^2}{4}\sum_i \nabla^2\left(\frac{Z}{r_i}\right)$$
$$H_{so} = \frac{Ze^2\hbar^2}{2m^2c^2r^3}\mathbf{l}.\mathbf{s} \tag{5}$$

and the rest are 2-body terms of spin and orbit interactions. $\mathbf{p_i}$ is the electron momentum, **L** and **S** are orbital and spin angular momenta. Program SS [59, 60] includes contributions of the three 1-body terms and the 2-body term of the Breit interaction (the first three spin–orbit interaction terms), and part of last three terms. BPRM codes [61, 62] include the 1-body terms.

Each relativistic correction term improves the accuracy of energy levels and hence transitions over the non-relativistic LS coupling energies and transitions. Hence, SS program improves accuracy by inclusion of the additional terms in comparison to BPRM method. However, accuracy can be enhanced faster with increment in configuration interaction than the correction terms. The R-matrix method incorporates much more configuration interaction than atomic structure calculations. Hence, R-matrix results are often more accurate than those of SS. One main difference in non-relativistic LS coupling and relativistic Breit–Pauli approximation is seen as having much more fine structure energy levels that belong to a single LS energy term. This leads to much more possible transitions among energy levels than a single one between two LS terms, and hence creation of a more accurate spectrum. The number of transitions is increases even more since selection rules for fine structure allows more transitions that are not possible in LS coupling. In addition, transitions occur among the fine structure levels belonging to a LS term which is not possible for a LS term. Hence, for accurate spectral features, relativistic approach is necessary.

In the BPRM method, the wavefunction expansion is expressed in close coupling (CC) approximation, where the atomic system is represented as a (N+1) number of electrons, N is the number of electrons in the core ion interacting with the (N+1)th electron. The total (e+ion) wave function, Ψ_E, in a symmetry $SL\pi$ is expressed as (e.g., [63])

$$\Psi_E\,(e+ion) = A\sum_i \chi_i\,(ion)\,\theta_i + \sum_j c_j\Phi_j \tag{6}$$

where χ_i is the core ion eigenfunction at the ground and various excited levels and the sum is over the number of core ion excitation considered for the atomic process. θ_i is the (N+1)th electron wave function with kinetic energy k_i^2 in a channel coupled with the core ion labeled as $S_iL_i\,(J_i)\,\pi_i k_i^2\,\ell_i\,[SL\,(J)\,\pi]$. A is the antisymmetrization operator. In the second term which is basically part of the first term, the Φ_js are bound channel functions of the (N+1)-electrons system that provides the orthogonality between the continuum and the bound electron orbitals and account for short range correlation. Substitution of $\Psi_E(e+ion)$ in the Schrodinger equation introduces a set of coupled equations that are solved by the R-matrix method. General descriptions of the R-matrix method can be found, e.g., in [57, 58, 63]. The energy eigenvalues from the R-matrix calculations are absolute and the (N+1)th electron can be bound or in the continuum depending on its negative or positive energy (E).

In contrast to BPRM, atomic structure calculations, such as using SS, compute energy values relative to the ground state, and does not specify whether the state is bound or in continuum. The wavefunction in SS is similar to the first term of CC expansion, but all core ion orbital functions are directly multiplied by the outer electron orbital and the sum is over the configurations producing a specific state and thus includes contributions of multiconfigurations interactions. Solutions of from SS calculations are given by Whittaker functions. Thomas–Fermi scaling parameters in SS calculations impacts on the expanding or compressing the orbital functions but maintains the right number of nodes and the orthogonality condition.

The probability for transition from state i to j, $P_{\rm ij}$, due to a photon absorption is given by (e.g., [63])

$$P_{\rm ij} = 2\pi\frac{c^2}{h^2\nu_{\rm ji}^2}|<j|\frac{e}{mc}\widehat{\mathbf{e}}.\mathbf{p}e^{i\mathbf{k}.\mathbf{r}}|i>|^2\rho\left(\nu_{\rm ji}\right) \tag{7}$$

where k is the wave vector, $\nu_{\rm ij}$ is the photon frequency for transition, ρ is the radiation density along with other standard constants. Various terms in $e^{i\mathbf{k}.\mathbf{r}}$ introduce various multipole transitions, such as, the first term gives the electric dipole transitions E1, the second term gives E2 and M1, and the third term E3 and M2. The general line strength of the transitions is obtained from

$$S^{\rm X\lambda}\,(ij) = \left|\left\langle\Psi_j||O^{\rm X\lambda}||\Psi_i\right\rangle\right|^2 \qquad S\,(ji) = S\,(ij) \tag{8}$$

where $O^{\rm X\lambda}$ is the operator for various transitions Xλ. We report transitions up to the third term. For E1 transitions, oscillator strengths, radiative decay rate which is also known as transition probability or Einstein's A-coefficient, and the corresponding photoabsorption cross sections can be obtained as

$$f_{\rm ij} = \frac{E_{ji}}{3g_i}S^{\rm E1}\,({\rm ij}), \quad A_{ji}^{\rm E1} = \alpha^3\frac{g_i}{g_j}E_{\rm ji}^2 f_{\rm ij}$$
$$\sigma_{PI}\,(\nu) = 8.064\frac{E_{ij}}{3g_i}S^{\rm E1}\,[Mb] \tag{9}$$

where $E_{\rm ji}$ is the transition energy, ν is the photon energy, and α is the fine structure constant, g_j and g_i being the statistical weights of the upper and lower states, respectively. The radiative decay rates for higher order multipole radiation electric quadrupole (E2) and magnetic dipole (M1) can be obtained as (e.g., [60])

$$g_jA_{ji}^{\rm E2} = 2.6733\times10^3{\rm s}^{-1}\left(E_j-E_i\right)^5S^{\rm E2}\,(i,j) \tag{10}$$

$$g_jA_{ji}^{\rm M1} = 3.5644\times10^4{\rm s}^{-1}\left(E_j-E_i\right)^3S^{\rm M1}\,(i,j) \tag{11}$$

and for electric octopole (E3) and magnetic quadrupole (M2) as

$$g_jA_{ji}^{\rm E3} = 1.2050\times10^{-3}{\rm s}^{-1}\left(E_j-E_i\right)^7S^{\rm E3}\,(i,j) \tag{12}$$

$$g_jA_{ji}^{\rm M2} = 2.3727\times10^{-2}{\rm s}^{-1}\left(E_j-E_i\right)^5S^{\rm M2}\,(i,j) \tag{13}$$

Table 1. The table presents levels and their energies (E_t) of core ions P II and P III that are included in the wave function expansion of P I and P II, respectively.

	P II				P III			
			E_t(Ry)	E_t(Ry)			E_t(Ry)	E_t(Ry)
	Level	J_t	NIST	SS	Level	J_t	NIST	SS
1	$3s^23p^2(^3P)$	0	0.0	0.	$3s^23p(^2P^o)$	1/2	0.0	0.
2	$3s^23p^2(^3P)$	1	0.00150	0.00199	$3s^23p(^2P^o)$	3/2	0.005095	0.00429
3	$3s^23p^2(^3P)$	2	0.00427	0.00562	$3s3p^2(^4P)$	5/2	0.523559	0.51278
4	$3s^23p^2(^1D)$	2	0.08094	0.10513	$3s3p^2(^4P)$	3/2	0.520570	0.51028
5	$3s^23p^2(^1S)$	0	0.19661	0.21350	$3s3p^2(^4P)$	1/2	0.518708	0.50874
6	$3s3p^3(^5S^o)$	2	0.41642	0.34507	$3s3p^2(^2D)$	3/2	0.682693	0.70551
7	$3s3p^3(^3D^o)$	3	0.59461	0.59151	$3s3p^2(^2D)$	5/2	0.682957	0.70565
8	$3s3p^3(^3D^o)$	2	0.59481	0.59117	$3s3p^2(^2S)$	1/2	0.913094	0.99414
9	$3s3p^3(^3D^o)$	1	0.59512	0.59102	$3s3p^2(^2P)$	1/2	0.993621	1.03335
10	$3s3p^3(^3P^o)$	2	0.69953	0.70112	$3s3p^2(^2P)$	3/2	0.997044	1.03613
11	$3s3p^3(^3P^o)$	1	0.69996	0.70162	$3s^23d(^2D)$	3/2	1.065039	1.14381
12	$3s3p^3(^3P^o)$	0	0.70006	0.70181	$3s^23d(^2D)$	5/2	1.065142	1.14392
13	$3s3p^3(^1D^o)$	2	0.70814	0.73277	$3s^24s(^2S)$	1/2	1.073800	1.10909
14	$3s^23p4s(^3P^o)$	2	0.78913	0.80961	$3s^24p(^2P^o)$	1/2	1.28832	1.34867
15	$3s^23p4s(^3P^o)$	1	0.79047	0.80536	$3s^24p(^2P^o)$	3/2	1.28956	1.34955
16	$3s^23p4s(^3P^o)$	0	0.79394	0.80394	$3p^3(^2D^o)$	3/2	1.342508	1.38637
17	$3s^23p3d(^3F^o)$	4	0.80013	0.82044	$3p^3(^2D^o)$	5/2	1.343073	1.38678
18	$3s^23p3d(^3F^o)$	3	0.80161	0.81777	$3p^3(^4S^o)$	3/2	1.455433	1.49071
19	$3s^23p3d(^3F^o)$	2	0.80366	0.81585				
20	$3s^23p4s(^1P^o)$	1	0.81005	0.82108				
21	$3s^23p4p(^1P)$	1	0.92617	1.03907				
22	$3s^23p3d(^1P^o)$	1	0.93677	0.96034				
23	$3s^23p3d(^3P^o)$	2	0.94434	0.97588				
24	$3s^23p3d(^3P^o)$	1	0.94549	0.97741				
25	$3s^23p3d(^3P^o)$	0	0.94717	0.97818				
26	$3s^23p3d(^3D^o)$	1	0.94818	1.00434				
27	$3s^23p3d(^3D^o)$	3	0.94821	1.00551				
28	$3s^23p3d(^3D^o)$	2	0.94865	1.0050				

Note: Calculated energies from SUPERSTRUCTURE (SS) are compared with those of Martin et al. [5] available in the NIST table [8]. NIST, National Institute of Standards and Technology.

While BPRM can generate a much larger set of transitions for n going up to $n = 10$, SS can compute transitions for n going to up to 5 or 6. The accuracy of SS is comparable to that of Dirac–Fock approximation for most ions. R-matrix can provide higher accuracy as it can accommodate a much larger set of configurations.

The lifetime of a level k can be computed as

$$\tau_k = \frac{1}{\sum_i A_{\rm ki}} \tag{14}$$

3. Computation

The oscillator strengths for P I and P II were obtained using the Breit–Pauli R-matrix package of codes [61, 62]. The computation involves a number of stages, named as, STG1, STG2, RECUPD, STGH, STGB, and STGBB. The first stage, STG1, is initiated with wavefunctions of the core ion as input and carry out various numerical integration. Atomic structure program SS [60] is used to obtain the core ion wavefunctions.

The CC wavefunction expansion, eq. (5), for P I included 28 levels of core ion P II, and that of P II 18 levels of core ion P III. A set of configurations for each core ion was optimized by program SS for the wave functions. The core ion levels and their calculated energies are presented in Table 1. The table compares the calculated SS energies of the core ions with the compiled energies of NIST [8]. The comparison shows agreement between the calculated and measured energies is within a few percent for most levels.

As Table 1 shows for both core ions, outer electron excitation included 3d, 4s, 4p orbitals. The final states of the (N+1)-electron system were obtained from these levels added by the angular momenta of the outer electron, ranging between $0 \le l \le 9$. Hence, the final states can be $n \le 10$. The second term of the wavefunction, eq. (6), included 87 configurations for P I and 39 configurations of P II.

STG2 and RECUPD carried out the angular algebra, and STGH computed the Hamiltonian matrix and dipole transition matrices. Computational details for P II oscillator

Table 2. Sets of optimized configurations and Thomas–Fermi scaling parameters (λ_{nl}) for the orbitals used to obtain the wavefunctions and energies of 15 phosphorus ions using program SUPERSTRUCTURE [60].

	P I
Configurations:	$1s^22s^22p^63s^23p^3$(1), $1s^22s^22p^63s^23p^24s$(2), $1s^22s^22p^63s3p^4$(3), $1s^22s^22p^63s^23p^24p$(4), $1s^22s^22p^63s^23p^23d$(5), $1s^22s^22p^63s^23p^24d$(6), $1s^22s^22p^63s^23p3d^2$(7), $1s^22s^22p^63s3p^33d$(8), $1s^22s^22p^63p^5$(9), $1s^22s^22p^63p^43d$(10)
λ_{nl}	1.40 (1s), 1.25 (2s), 1.20 (2p), 1.27 (3s), 1.02 (3p), 1.19 (3d), 1.20 (4s), 0.98 (4p), 1.17 (4d)
	P II
Configurations:	$1s^22s^22p^63s^23p^2$(1), $1s^22s^22p^63s3p^3$(2), $1s^22s^22p^63s^23p3d$(3), $1s^22s^22p^63s^23p4s$(4), $1s^22s^22p^63s^23p4p$(5), $1s^22s^22p^63s^23p4d$(6), $1s^22s^22p^63s^23p4f$(7), $1s^22s^22p^63s^23p5s$(8), $1s^22s^22p^63s3p^23d$(9), $1s^22s^22p^63p^4$(10), $1s^22s^22p^63s^23d^2$(11), $1s^22s^22p^63s^23d4s$(12), $1s^22s^22p^63p^34s$(13), $1s^22s^22p^63s3p3d^2$(14)
λ_{nl}	1.42 (1s), 1.25 (2s), 1.18 (2p), 1.15 (3s), 1.1 (3p), 1.0 (3d), 1.3 (4s), 0.97 (4p), 1.0 (4d), 1.0 (4f), 1.0 (5s)
	P III
Configurations:	$1s^22s^22p^63s^23p$(1), $1s^22s^22p^63s3p^2$(2), $1s^22s^22p^63s^23d$(3), $1s^22s^22p^63s^24s$(4), $1s^22s^22p^63s^24p$(5), $1s^22s^22p^63p^3$(6), $1s^22s^22p^63s3p3d$(7), $1s^22s^22p^63s^24d$(8), $1s^22s^22p^63s^24f$(9), $1s^22s^22p^63s^25s$(10), $1s^22s^22p^63s3p4s$(11), $1s^22s^22p^63s3p4p$(12), $1s^22s^22p^63s3p4d$(13), $1s^22s^22p^63s3p4f$(14), $1s^22s^22p^63p^23d$(15), $1s^22s^22p^63p^24s$(16), $1s^22s^22p^63p^24p$(17), $1s^22s^22p^63p^24d$(18), $1s^22s^22p^63p^24f$(19)
λ_{nl}	1.1 (1s), 1.0 (2s), 1.0 (2p), 1.0 (3s), 1.0 (3p), 1.0 (3d), 1.1 (4s), 1.0 (4p), 1.0 (4d), 1.0 (4f),1.0 (5s), 1.0 (5p)
	P IV
Configurations:	$1s^22s^22p^63s^2$(1), $1s^22s^22p^63s3p$(2), $1s^22s^22p^63s3d$(3), $1s^22s^22p^63s4s$(4), $1s^22s^22p^63s4p$(5), $1s^22s^22p^63s4d$(6), $1s^22s^22p^63s4f$(7), $1s^22s^22p^63p^2$(8), $1s^22s^22p^63p3d$(9), $1s^22s^22p^63p4s$(10), $1s^22s^22p^63p4p$(11), $1s^22s^22p^63p4d$(12), $1s^22s^22p^63p4f$(13), $1s^22s^22p^63d^2$(14), $1s^22s^22p^63s5s$(15), $1s^22s^22p^63s5p$(16), $1s^22s^22p^63s5d$(17), $1s^22s^22p^63s5f$(18),
λ_{nl}	2.0 (1s), 1.0 (2s), 1.0 (2p), 1.0 (3s), 1.0 (3p), 1.0 (3d), 1.1 (4s), 1.0 (4p), 1.0 (4d), 1.0 (4f),1.0 (5s), 1.0 (5p), 1.0 (5d), 1.0 (5f)
	P V
Configurations:	$1s^22s^22p^63s$(1), $1s^22s^22p^63p$(2), $1s^22s^22p^63d$(3), $1s^22s^22p^64s$(4), $1s^22s^22p^64p$(5), $1s^22s^22p^64d$(6), $1s^22s^22p^64f$(7), $1s^22s^22p^53s^2$(8), $1s^22s^22p^65s$(9), $1s^22s^22p^65p$(10), $1s^22s^22p^65d$(11), $1s^22s^22p^65f$(12), $1s^22s^22p^65g$(13), $1s^22s^22p^43s^23p$(14), $1s^22s^22p^43s^23d$(15), $1s^22s^22p^53s3p$(16), $1s^22s^22p^53s3d$(17), $1s^22s^22p^53s4s$(18), $1s^22s^22p^53s4p$(19), $1s^22s^22p^53s4d$(20),
λ_{nl}	1.30 (1s), 1.30 (2s), 0.998 (2p), 1.20 (3s), 0.998 (3p), 0.91 (3d), 1.10 (4s), 0.99 (4p), 0.995 (4d), 1.0 (4f), 1.0 (5s), 1.0 (5p), 1.0 (5d), 1.0 (5f), 1.0 (5g)
	P VI
Configurations:	$1s^22s^22p^6$(1), $1s^22s^22p^53s$(2), $1s^22s^22p^53p$, $1s^22s^22p^53d$(3), $1s^22s^22p^54s$(4), $1s^22s^22p^54p$(5), $1s^22s^22p^54d$(6), $1s^22s^22p^54f$(7), $1s^22s^22p^55s$(8), $1s^22s^22p^55p$(9), $1s^22s^22p^55d$(10), $1s^22s^22p^55f$(11), $1s^22s^22p^55g$(12), $1s^22s^22p^43s^2$(13), $1s^22s^22p^43s3p$(14), $1s^22s^22p^43s3d$(15), $1s2s^22p^63s$(16), $1s2s^22p^63p$(17)
λ_{nl}	1.30 (1s), 1.30 (2s), 0.998 (2p), 1.20 (3s), 0.998 (3p), 0.91 (3d), 1.10 (4s), 0.99 (4p), 0.995 (4d), 1.0 (4f),1.0 (5s), 1.0 (5p), 1.0 (5d), 1.0 (5f), 1.0 (5g)
	P VII
Configurations:	$1s^22s^22p^5$(1), $1s^22s2p^6$(2), $1s^22s^22p^43s$(3), $1s^22s^22p^43p$(4), $1s^22s^22p^43d$(5), $1s^22s^22p^44s$(6), $1s^22s^22p^44p$(7), $1s^22s^22p^44d$(8), $1s^22s^22p^44f$(9), $1s^22s^22p^45s$(10), $1s^22s^22p^45p$(11), $1s^22s^22p^45d$(12), $1s^22s^22p^45f$(13), $1s^22s^22p^45g$(14), $1s^22s2p^53s$(15), $1s^22s2p^53p$(16), $1s^22s2p^53d$(17), $1s^22s2p^54s$(18), $1s^22s2p^54p$(19), $1s^22s2p^54d$(20), $1s2s^22p^6$(21), $1s2s^22p^53s$(22), $1s2s^22p^53p$(23)
λ_{nl}	1.30 (1s), 1.20 (2s), 1.15 (2p), 1.10 (3s), 1.10 (3p), 1.10 (3d), 1.0 (4s), 1.0 (4p), 1.0 (4d), 1.0 (4f), 1.0 (5s), 1.0 (5p),1.0 (5d), 1.0 (5f), 1.0 (5g)

Table 2. (*continued*).

	P VIII
Configurations:	$1s^2 2s^2 2p^4$(1), $1s^2 2s2p^5$(2), $1s^2 2p^6$(3), $1s^2 2s^2 2p^3 3s$(4), $1s^2 2s^2 2p^3 3p$(5), $1s^2 2s^2 2p^3 3d$(6), $1s^2 2s^2 2p^3 4s$(7), $1s^2 2s^2 2p^3 4p$(8), $1s^2 2s^2 2p^3 4d$(9), $1s^2 2s^2 2p^3 4f$(10), $1s^2 2s^2 2p^3 5s$(11), $1s^2 2s^2 2p^3 5p$(12), $1s^2 2s^2 2p^3 5d$(13), $1s^2 2s^2 2p^3 5f$(14), $1s^2 2s^2 2p^3 5g$(15), $1s^2 2s2p^4 3s$(16), $1s^2 2s2p^4 3p$(17), $1s^2 2s2p^4 3d$(18), $1s^2 2s2p^4 4s$(19), $1s^2 2s2p^4 4p$(20), $1s^2 2s2p^4 4d$(21), $1s^2 2s^2 2p^2 3s^2$(22), $1s2s^2 2p^5$(23), $1s2s^2 2p^4 3s$(24), $1s2s^2 2p^4 3p$(24)
λ_{nl}	1.30 (1s), 1.17 (2s), 1.12 (2p), 0.95 (3s), 1.03 (3p), 1.0 (3d), 1.0 (4s), 1.0 (4p), 1.0 (4d), 1.0 (4f), 1.0 (5s), 1.0 (5p), 1.0 (5d), 1.0 (5f), 1.0 (5g)
	P IX
Configurations:	$1s^2 2s^2 2p^3$(1), $1s^2 2s2p^4$(2), $1s^2 2s^2 2p^2 3s$(3), $1s^2 2s^2 2p^2 3p$(4), $1s^2 2s^2 2p^2 3d$(5), $1s^2 2s^2 2p^2 4s$(6), $1s^2 2s^2 2p^2 4p$(7), $1s^2 2s^2 2p^2 4d$(8), $1s^2 2s^2 2p^2 4f$(9), $1s^2 2s^2 2p^2 5s$(10), $1s^2 2s^2 2p^2 5p$(11), $1s^2 2s^2 2p^2 5d$(12), $1s^2 2s^2 2p^2 5f$(13), $1s^2 2s^2 2p^2 5g$(14), $1s^2 2p^5$, $1s^2 2s2p^3 3s$(15), $1s^2 2s2p^3 3p$(16), $1s^2 2s2p^3 3d$(17), $1s2s^2 2p^4$(18), $1s2s^2 2p^3 3s$(19), $1s2s^2 2p^3 3p$(20)
λ_{nl}	1.35 (1s), 1.25 (2s), 1.15 (2p), 1.20 (3s), 1.15 (3p), 1.10 (3d), 1.0 (4s), 1.0 (4p), 1.0 (4d), 1.0 (4f), 1.0 (5s), 1.0 (5p), 1.0 (5d), 1.0 (5f), 1.0 (5g)
	P X
Configurations:	$1s^2 2s^2 2p^2$(1), $1s^2 2s2p^3$(2), $1s^2 2p^4$(3), $1s^2 2s^2 2p3s$(4), $1s^2 2s^2 2p3p$(5), $1s^2 2s^2 2p3d$(6), $1s^2 2s^2 2p4s$(7), $1s^2 2s^2 2p4p$(8), $1s^2 2s^2 2p4d$(9), $1s^2 2s^2 2p4f$(10), $1s^2 2s^2 2p5s$(11), $1s^2 2s^2 2p5p$(12), $1s^2 2s^2 2p5d$(13), $1s^2 2s^2 2p5f$(14), $1s^2 2s^2 2p5g$(15), $1s^2 2s2p^2 3s$(16), $1s^2 2s2p^2 3p$(17), $1s^2 2s2p^2 3d$(18), $1s^2 2s2p^2 4s$(19), $1s^2 2s2p^2 4p$(20), $1s^2 2s2p^2 4d$(21), $1s2s^2 2p^3$(22), $1s2s^2 2p^2 3s$(23), $1s2s^2 2p^2 3p$(24)
λ_{nl}	1.42 (1s), 1.25 (2s), 1.15 (2p), 1.25 (3s), 1.15 (3p), 1.17 (3d), 1.20 (4s), 1.20 (4p), 1.2 (4d), 1.0 (4f),1.0 (5s), 1.0 (5p), 1.0 (5d), 1.0 (5f), 1.0 (5g)
	P XI
Configurations:	$1s^2 2s^2 2p$(1), $1s^2 2s2p^2$(2), $1s^2 2p^3$(3), $1s^2 2s^2 3s$(4), $1s^2 2s^2 3p$(5), $1s^2 2s^2 3d$(6), $1s^2 2s2p3s$(7), $1s^2 2s2p3p$(8), $1s^2 2s2p3d$(9), $1s^2 s^2 4s$(10), $1s^2 s^2 4p$(11), $1s^2 s^2 4d$(12), $1s^2 s^2 4f$(13), $1s^2 s^2 5s$(14), $1s^2 s^2 5p$(15), $1s^2 s^2 5d$(16), $1s^2 s^2 5f$(17), $1s^2 s^2 5g$(18), $1s^2 2s2p4s$(19), $1s^2 2s2p4p$(20), $1s^2 2s2p4d$(21), $1s^2 2s3d^2$(22), $1s^2 2p^2 3s$(23), $1s^2 2p^2 3p$(24), $1s^2 2p^2 3d$(25), $1s^2 2p^2 4s$(26), $1s^2 2p^2 4p$(27), $1s2s^2 2p^2$(28), $1s2s^2 2p3s$(29), $1s2s^2 2p3p$(30), $1s2s^2 2p3d$(31)
λ_{nl}	2.50 (1s), 1.20 (2s), 1.02 (2p), 1.12 (3s), 1.10 (3p), 1.10 (3d), 1.10 (4s), 1.10 (4p), 1.0 (4d), 1.0 (4f),1.0 (5s), 1.0 (5p), 1.0 (5d), 1.0 (5f), 1.0 (5g)
	P XII
Configurations:	$1s^2 2s^2$(1), $1s^2 2s2p$(2), $1s^2 2s$(3), $1s^2 2s3s$(4), $1s^2 2s3p$(5), $1s^2 2s3d$(6), $1s^2 2s4s$(7), $1s^2 2s4p$(8), $1s^2 2s4d$(9), $1s^2 2s4f$(10), $1s^2 2p3s$(11), $1s^2 2p3p$(12), $1s^2 2p3d$(13), $1s^2 2p4s$(14), $1s^2 2p4p$(15), $1s^2 2p4d$(16), $1s^2 2p4f$(17), $1s^2 2s5s$(18), $1s^2 2s5p$(19), $1s^2 2s5d$(20), $1s^2 2s5f$(21), $1s^2 2s5g$(22), $1s^2 2p5s$(23), $1s2p5p$(24), $1s2p5d$(25), $1s2p5f$(26), $1s2p5g$(27), $1s2s^2 3s$(28), $1s2s^2 3p$(29), $1s^2 2p^2$(30), $1s^2 3s^2$(31), $1s^2 3p^2$(32), $1s^2 3d^2$(33)
λ_{nl}	1.38 (1s), 1.20 (2s), 1.08 (2p), 1.15 (3s), 1.01 (3p), 1.0 (3d), 1.0 (4s), 1.0 (4p), 1.0 (4d), 1.0 (4f), 1.0 (5s), 1.0 (5p),1.0 (5d), 1.0 (5f), 1.0 (5g)
	P XIII
Configurations:	$1s^2 2s$(1), $1s^2 2p$(2), $1s^2 3s$(3), $1s^2 3p$(4), $1s^2 3d$(5), $1s^2 4s$(6), $1s^2 4p$(7), $1s^2 4d$(8), $1s^2 4f$(9), $1s2s^2$(10), $1s2s2p$(11), $1s2s3s$(12), $1s2s3p$(13), $1s2s3d$(14), $1s2s4s$(15), $1s2s4p$(16), $1s2s4d$(17), $1s2s4f$(18), $1s2s5s$(19), $1s2s5p$(20), $1s2s5d$(21), $1s2s5f$(22), $1s2s5g$(23), $1s2p3s$(24), $1s2p3p$(25), $1s2p3d$(26), $1s2p4s$(27), $1s2p4p$(28), $1s2p^2$(29), $1s3s^2$(30), $1s3p^2$(31), $1s3d^2$(32)
λ_{nl}	1.30 (1s), 1.30 (2s), 0.998 (2p), 1.20 (3s), 0.998 (3p), 0.91 (3d), 1.10 (4s), 0.99 (4p), 0.995 (4d), 1.0 (4f),1.0 (5s), 1.0 (5p), 1.0 (5d), 1.0 (5f), 1.0 (5g)

Table 2. (*concluded*).

	P XIV
Configurations:	$1s^2(1)$, $1s2s(2)$, $1s2p(3)$, $1s3s(4)$, $1s3p(5)$, $1s3d(6)$, $1s4s(7)$, $1s4p(8)$, $1s4d(9)$, $1s4f(10)$, $2s^2(11)$, $2p^2(12)$, $2s^2(13)$, $3p^2(14)$, $3d^2(15)$, $2s2p(16)$, $2s3s(17)$, $2s3p(18)$, $2s3d(19)$, $2s4s(20)$, $2s4p(21)$, $2s4d(22)$, $2s4f(23)$, $2p3s(24)$, $2p3p(25)$, $2p3d(26)$, $2p4s(27)$, $2p4p(28)$
λ_{nl}	1.1 (1s), 1.0 (2s), 1.0 (2p), 1.0 (3s), 1.0 (3p), 1.0 (3d), 1.0 (4s), 1.0 (4p), 1.0 (4d), 1.0 (4f), 1.0 (5s), 1.0 (5p)
	P XV
Configurations:	$1s(1)$, $2s(2)$, $2p(3)$, $3s(4)$, $3p(5)$, $3d(6)$, $4s(7)$, $4p(8)$, $4d(9)$, $4f(10)$
λ_{nl}	1.0 (1s), 1.0 (2s), 1.0 (2p), 1.0 (3s), 1.0 (3p), 1.0 (3d), 1.0 (4s), 1.0 (4p), 1.0 (4d), 1.0 (4f), 1.0 (5s), 1.0 (5p)

Note: In the complete energy tables, configurations are specified by their numbers as given within the parenthesis next to them in the table.

strengths are similar to those for photoionization of the ion described in [21].

STGB computed the bound states and energies for P I and P II. Energy eigen values of the Hamiltonian matrix were obtained using fine energy meshes to search for the poles. BPRM codes do not identify the energy states. Spectroscopic identifications of the states were carried out using an algorithm based on quantum defect theory and angular algebra built in a code PRCBPID by Nahar [64, 65].

Program STGBB of the BPRM codes [62] was used to compute oscillator strengths. The energies and oscillators were processed using code PBPRAD [66] and the synthetic spectra were produced using code SPECTRA [67].

As mentioned above, the transition parameters for other P ions, including forbidden transitions of P I and P II, were obtained through atomic structure calculations using the later version of the program SS [60]. For each ion, an optimized set of configurations was selected such that it would include photo-excitation of low to high temperature plasma. SS typically accommodates transitions among configurations with principle quantum number n going up to 6. Optimization was carried out for an overall good agreement of the computed energies with those in NIST compilation table. We varied the Thomas–Fermi scaling parameters λ_{nl} of the orbital wavefunctions for optimization. Each configuration was treated spectroscopic, that is, all configurations were optimized for the best energies. The focus was on improving energies more in the low to intermediate range levels. The final optimized set of configurations and Thomas–Fermi λ_{nl} parameters are presented in Table 2.

All SS data were processed using code PRCSS [68]. The spectra of the ion were obtained using the code SPECTRA [67] that collected A-values of all dipole allowed transitions and computed the photoabsorption cross sections. It also added all cross sections corresponding to same transition wavelengths. The lifetimes of all levels of each ion were processed using program LIFETMSS [69] which used A-values of all transitions, dipole allowed and forbidden, to computed the lifetimes.

4. Results and discussions

We present very large sets of atomic data for energies, transition parameters (f, S, A-values), lifetimes, and the spectral features in various wavelength ranges from X-ray to IR for all 15 ionization stages of phosphorus, P I–P XV. In addition to providing accurate atomic data, one primary objective of the present study is finding wavelength ranges in which prominent spectral features and strong lines exist in P ions and hence can be used for search and identification of this biosignature element in the spectra of exoplanets or in any astronomical objects. An observed line can be identified if the transitional levels are known. However, to predict whether a line can be observed depends on the strength of the transition probability, assuming the line is not affected by the environmental factors.

Energies and transition parameters for the two ions, P I and P II, have been obtained using the relativistic BPRM method while those for ions P III–P XV have been obtained in relativistic Breit–Pauli approximation using atomic structure code SS. We have computed lifetimes of all excited levels using A-values obtained from BPRM method for P I and P II, and from SS for P III–P XV. SS has been used for atomic parameters of P I and P II as well, but we suggest use of BPRM results of P I and P II because of the higher accuracy of the method, and use of SS results only for forbidden transitions which the computer package of BPRM method does not compute.

We may mention that BPRM package of codes calculates bound levels with n going up to 10. Hence, the spectral lines and features for P I and P II correspond to bound–bound transitions only. On the other hand, SS computes all possible bound and continuum energy levels arise from the given set of configurations. Typically, the high lying levels from SS exist in the continuum. Hence, the spectral features includes photoabsorption lines for both bound–bound and bound–continuum transitions. The continuum levels, beyond the ionization threshold, are the Rydberg autoionizing states, and the transitions to continuum appear as resonances in photoionization cross sections. These lines can be seen observed when they are strong and isolated. Since SS computes the energy of an continuum level as an eigenvalue, the resonance is a single point without the typical broadened Lorentzian profile.

Accuracy checks of the present atomic parameters for the spectral features have been carried out in a number of ways. The atomic data have been benchmarked by comparing them with available calculated and measured values of

energies, transition probabilities, and radiative lifetimes. Radiative lifetime of a level is the reciprocal of sum of transition probabilities from the level to its lower levels. It is a measurable quantity in laboratories and often measured with high precision. Hence, lifetimes are commonly used for determination of accuracy of transition probabilities. Accuracy analysis of the present work indicates that the present spectral features can provide dependable guidance for search of phosphorus.

We compare our energies of P I–P XIV in Table 3 with the measured values by Martin et al. [5] and of P XV with those by Yerokhin and Shamaev [6] and Erickson [7] all of which are listed at NIST [8] table. For brevity, we chose 10 levels of each ion to compare, and all comparisons are placed in the same Table 3. The table lists the total number of levels obtained for each ion. Most of our energies compared in Table 3 are in excellent agreement, less than 1 to a few percent, with the measured values. Complete tables of energies will be available online at NORAD-Atomic-Data database [26]. In the complete table of energies from BPRM method, the configurations with the levels are provided. In the energy tables from SS, the configuration numbers for the levels are specified. These numbers are the configuration numbers specified within parenthesis in Table 2. The list of configurations of Table 2 is also given inside the energy data files.

We discuss the atomic data for transition probabilities, lifetimes, and spectral features of each ion separately in the subsections below. However, for brevity with 15 ions of phosphorus, we provide short tables of examples of atomic data along with comparison with others for each ion. We have combined the short tables for the 15 phosphorus ions (P I through P XV) into one table, similar to the energy table, for each quantity of transition probabilities and lifetimes. This provides an overall picture of the ionization stages of the element.

4.1. P I

We have obtained from BPRM method 343 and from SS 245 fine structure energy levels of P I, as specified in Table 3. We find good agreement in energies, BPRM energies slightly better than those from SS, with measured energies of Martin et al. [5]. The set of nine configurations for P I in SS calculations produced 245 levels, including both bound and continuum. Being neutral P I was a very sensitive ion for optimization of the configurations using SS.

We present 32 678 dipole allowed (E1) transitions calculated from the BPRM method. A number of transitions along with comparison with existing values available in NIST [8] compiled table are presented in Table 4. For the first dipole allowed transitions, $3s^2 3p^3(^4S^o) - 3s^2 3p^2 4s(^4P)$, the present A-values from BPRM method have good agreement with those of Lawrence [9] and Fischer et al. [12]. However, for the second set of E1 transitions, $3s^2 3p^3(^4S^o) - 3s3p^4(^4P)$, there seem to be general disagreement among the groups. For the rest of the transitions, the present radiative decay rates show general agreement with refs. [9, 12] for allowed transitions.

We have computed a smaller set of E1 transitions, a total of 8726, using SS. This set includes both the bound–bound and bound–continuum transitions. Improvement of this set required significant amount of optimization because of the sensitivity in slight changes in the orbital wavefunctions over the E1 transition parameters. E1 transitions obtained from SS are also compared in Table 4. Comparison shows general agreement.

We compare the forbidden E2 and M1 transitions obtained from SS with those available in the NIST table, calculated by Czyzak and Krueger [10]. Comparison shows better agreement between the present and those of ref. [10] for the E2 transitions while present values for M1 transitions are lower than those of ref. [10]. For confirmation of higher accuracy these transitions in P I need further study in the future. We suggest use of BPRM values for E1 transitions which correspond to a much larger set of bound levels, and SS values for forbidden transitions.

Lifetimes of a number of levels of P I were measured using beam–foil technique by Curtis et al. [13] and using fluorescence detection technique by Berzinish et al. [14]. Present calculated lifetimes computed using A-values from BPRM method are compared with measured values in Table 5. We find excellent agreement with the measured values and other theoretical values by Froese-Fischer et al. [12].

Features of photoabsorption spectrum of P I is presented in Fig. 1. Panel (*a*) shows the spectrum going up to 1×10^6 Å; wavelengths covering most of the strong lines of P I. The figure shows the wavelength regions of strengths, particularly up to far IR region of 4.5×10^5 Å; that dominate the spectrum. It is somewhat surprising that the strengths of lines continue to remain strong at 1M (Å), although density of strong lines has become sparse. The upper panel (*b*) elaborates the spectrum up to 31 000 (Å), within the range for JWST, presenting wavelength regions of strong line strength. This includes optical and IR regions. However, the strengths are lower than those in the far-IR regions.

4.2. P II

We have obtained for P II, 475 bound fine structure levels from BPRM method and 243 bound and continuum levels from SS. The BPRM energy levels are from the 18 levels of the core ion combining with the outer electron of angular momenta $l = 0$–9 and $n \leq 10$. A small set of energy levels from both approaches are listed in Table 3 and compared with those of measured by Martin et al. [5] and available in NIST [8]. BPRM values are slightly higher and SS values are slightly lower than the measured values. The overall agreement of them with the measured values is in general good. With inclusion of more configuration interactions, as explained for the case of P I, the wavefunctions for BPRM method are expected to be more accurate.

We have obtained a larger set of E1 transitions, 23 255, from BPRM method compared to 7920 from SS and 27 172 forbidden transitions from SS. Limited number of transitions were studied by a number of investigators. Comparison is made with them in Table 4. With similar reasons given for P I, we suggest use of BPRM transitions for P II which are expected to be more accurate. A-values for the forbidden transitions should be used from SS calculations.

Table 3. Comparison of the present calculated energies for the fine structure levels of P I–P XV with those of Martin et al. [5] available in the compilation table of the National Institute of Standards and Technology (NIST) [8].

P I: $N_{BPRM} = 543$, $N_{SS} = 245$						
K	Configuration	Level	J	E_{NIST}(Ry)	E_{SS}(Ry)	E_{BPRM}(Ry)
1	$3s^2 3p^3$	$^4S^o$	3/2	0	0	0.
2	$3s^2 3p^3$	$^2D^o$	3/2	0.10367	0.11415	0.1108
3	$3s^2 3p^3$	$^2D^o$	5/2	0.10353	0.11417	0.1106
4	$3s^2 3p^3$	$^2P^o$	1/2	0.17084	0.16936	0.17413
5	$3s^2 3p^3$	$^2P^o$	3/2	0.17061	0.16937	0.17429
6	$3s^2 3p^2 4s$	$^4P^o$	1/2	0.52352	0.48482	0.53221
7	$3s^2 3p^2 4s$	^4P	3/2	0.52369	0.48520	0.53361
8	$3s^2 3p^2 4s$	^4P	5/2	0.52393	0.52470	0.53594
9	$3s^2 3p^2 4s$	^2P	1/2	0.55908	0.54172	0.5516
10	$3s^2 3p^2 4s$	^2P	3/2	0.56001	0.54256	0.55444
P II, $N_{BPRM} = 475$, $N_{SS} = 243$						
K	Configuration	Level	J	E_{SS}(Ry)	E_{NIST}(Ry)	E_{BPRM}(Ry)
1	3s23p2	^3Pe	0.0	0.000E+00	0.000E+00	0.000E+00
2	3s23p2	^3Pe	1.0	1.232E-03	1.503E-03	1.370E-03
3	3s23p2	^3Pe	2.0	3.554E-03	4.275E-03	3.920E-03
4	3s23p2	^1De	2.0	1.030E-01	8.094E-02	8.554E-02
5	3s23p2	^1Se	0.0	2.013E-01	1.966E-01	2.269E-01
6	3s3p3	^5So	2.0	3.063E-01	4.164E-01	4.237E-01
7	3s3p3	^3Do	1.0	5.835E-01	5.946E-01	6.190E-01
8	3s3p3	^3Do	2.0	5.836E-01	5.948E-01	6.192E-01
9	3s3p3	^3Do	3.0	5.837E-01	5.951E-01	6.196E-01
10	3s3p3	^3Po	2.0	7.602E-01	6.995E-01	7.476E-01
P III, $N_{SS} = 235$						
K	Configuration	Level	J	E_{SS}(Ry)	E_{NIST}(Ry)	
1	3s23p	^2Po	0.5	0.000E+00	0.000E+00	
2	3s23p	^2Po	1.5	4.290E-03	5.095E-03	
3	3s3p2	^4Pe	0.5	5.087E-01	5.187E-01	
4	3s3p2	^4Pe	1.5	5.102E-01	5.206E-01	
5	3s3p2	^4Pe	2.5	5.128E-01	5.236E-01	
6	3s3p2	^2De	1.5	7.056E-01	6.827E-01	
7	3s3p2	^2De	2.5	7.056E-01	6.830E-01	
8	3s3p2	^2Se	0.5	9.941E-01	9.131E-01	
9	3s3p2	^2Pe	0.5	1.0333+00	9.936E-01	
10	3s3p2	^2Pe	1.5	1.036E+00	9.970E-01	
P IV, $N_{SS} = 101$						
K	Configuration	Level	J	E_{SS}(Ry)	E_{NIST}(Ry)	
1	2p63s2	^1Se	0.0	0.000E+00	0.000E+00	
2	3s3p	^3Po	0.0	6.081E-01	6.189E-01	
3	3s3p	^3Po	1.0	6.101E-01	6.210E-01	
4	3s3p	^3Po	2.0	6.140E-01	6.253E-01	
5	3s3p	^1Po	1.0	9.815E-01	9.586E-01	
6	3p2	^1De	2.0	1.435E+00	1.441E+00	
7	3p2	^3Pe	0.0	1.504E+00	1.503E+00	
8	3p2	^3Pe	1.0	1.506E+00	1.505E+00	
9	3p2	^3Pe	2.0	1.510E+00	1.510E+00	
10	3s3d	^3De	1.0	1.747E+00	1.726E+00	
P V, $N_{SS} = 161$						
K	Configuration	Level	J	E_{SS}(Ry)	E_{NIST}(Ry)	
1	2p63s	^2Se	0.5	0.000E+00	0.000E+00	
2	2p63p	^2Po	0.5	8.001E-01	8.077E-01	

Table 3. (*continued*).

P V, N_{SS} = 161					
K	Configuration	Level	J	E_{SS}(Ry)	E_{NIST}(Ry)
3	2*p*63*p*	^2Po	1.5	8.073E-01	8.151E-01
4	2*p*63*d*	^2De	1.5	1.843E+00	1.861E+00
5	2*p*63*d*	^2De	2.5	1.844E+00	1.861E+00
6	2*p*64*s*	^2Se	0.5	2.454E+00	2.487E+00
7	2*p*64*p*	^2Po	0.5	2.742E+00	2.772E+00
8	2*p*64*p*	^2Po	1.5	2.745E+00	2.774E+00
9	2*p*64*d*	^2De	1.5	3.117E+00	3.147E+00
10	2*p*64*d*	^2De	2.5	3.117E+00	3.147E+00
P VI, N_{SS}=168					
K	Configuration	Level	J	E_{SS}(Ry)	E_{NIST}(Ry)
1	2*s*22*p*6	^1Se	0.0	0.000E+00	0.000E+00
2	2*s*22*p*53*s*	^3Po	2.0	9.795E+00	9.931E+00
3	2*s*22*p*53*s*	^3Po	1.0	9.829E+00	9.963E+00
4	2*s*22*p*53*s*	^3Po	0.0	9.872E+00	9.997E+00
5	2*s*22*p*53*s*	^1Po	1.0	9.921E+00	1.005E+01
6	2*s*22*p*53*p*	^3Se	1.0	1.061E+01	1.068E+01
7	2*s*22*p*53*p*	^3De	3.0	1.072E+01	1.080E+01
8	2*s*22*p*53*p*	^3De	2.0	1.073E+01	1.081E+01
9	2*s*22*p*53*p*	^3De	1.0	1.075E+01	1.084E+01
10	2*s*22*p*53*p*	^3Pe	2.0	1.079E+01	1.092E+01
P VII, N_{SS}=386					
K	Configuration	Level	J	E_{SS}(Ry)	E_{NIST}(Ry)
1	2*s*22*p*5	^2Po	1.5	0.000E+00	0.000E+00
2	2*s*22*p*5	^2Po	0.5	8.581E-02	6.628E-02
3	2*s*2*p*6	^2Se	0.5	4.327E+00	4.144E+00
4	2*s*22*p*4(3*P*)3*s*	^4Pe	2.5	1.133E+01	1.148E+01
5	2*s*22*p*4(3*P*)3*s*	^4Pe	1.5	1.137E+01	1.152E+01
7	2*s*22*p*4(3*P*)3*s*	^2Pe	1.5	1.150E+01	1.164E+01
8	2*s*22*p*4(3*P*)3*s*	^2Pe	0.5	1.155E+01	1.169E+01
9	2*s*22*p*4(1*D*)3*s*	^2De	2.5	1.188E+01	1.200E+01
10	2*s*22*p*4(1*D*)3*s*	^2De	1.5	1.188E+01	1.200E+01
P VIII, N_{SS}=653					
K	Configuration	Level	J	E_{SS}(Ry)	E_{NIST}(Ry)
1	2*s*22*p*4	^3Pe	2.0	0.000E+00	0.000E+00
2	2*s*22*p*4	^3Pe	1.0	6.271E-02	5.249E-02
3	2*s*22*p*4	^3Pe	0.0	8.482E-02	7.128E-02
4	2*s*22*p*4	^1De	2.0	5.100E-01	4.762E-01
5	2*s*22*p*4	^1Se	0.0	1.018E+00	1.010E+00
6	2*s*2*p*5	^3Po	2.0	3.753E+00	3.680E+00
7	2*s*2*p*5	^3Po	1.0	3.811E+00	3.726E+00
8	2*s*2*p*5	^3Po	0.0	3.841E+00	3.752E+00
9	2*s*2*p*5	^1Po	1.0	5.302E+00	5.108E+00
10	2*p*6	^1Se	0.0	8.921E+00	8.598E+00
P IX, N_{SS} = 498					
K	Configuration	Level	J	E_{SS}(Ry)	E_{NIST}(Ry)
1	2*s*22*p*3	^4So	1.5	0.000E+00	0.000E+00
2	2*s*22*p*3	^2Do	1.5	7.258E-01	6.916E-01
3	2*s*22*p*3	^2Do	2.5	7.400E-01	6.969E-01
4	2*s*22*p*3	^2Po	0.5	1.077E+00	1.058E+00
5	2*s*22*p*3	^2Po	1.5	1.093E+00	1.067E+00
6	2*s*2*p*4	^4Pe	2.5	3.153E+00	3.148E+00
7	2*s*2*p*4	^4Pe	1.5	3.207E+00	3.193E+00

Table 3. (*continued*).

P IX, $N_{SS} = 498$					
K	Configuration	Level	J	E_{SS}(Ry)	E_{NIST}(Ry)
8	2*s*2*p*4	^4Pe	0.5	3.236E+00	3.217E+00
9	2*s*2*p*4	^2De	1.5	4.436E+00	4.331E+00
10	2*s*2*p*4	^2De	2.5	4.439E+00	4.332E+00
P X, $N_{SS} = 430$					
K	Configuration	Level	J	E_{SS}(Ry)	E_{NIST}(Ry)
1	2*s*22*p*2	^3Pe	0.0	0.000E+00	0.000E+00
2	2*s*22*p*2	^3Pe	1.0	4.111E-02	3.364E-02
3	2*s*22*p*2	^3Pe	2.0	1.026E-01	8.242E-02
4	2*s*22*p*2	^1De	2.0	5.870E-01	5.439E-01
5	2*s*22*p*2	^1Se	0.0	1.119E+00	1.093E+00
6	2*s*2*p*3	^5So	2.0	1.481E+00	1.529E+00
7	2*s*2*p*3	^3Do	2.0	3.003E+00	2.945E+00
8	2*s*2*p*3	^3Do	1.0	3.004E+00	2.947E+00
9	2*s*2*p*3	^3Do	3.0	3.010E+00	2.946E+00
10	2*s*2*p*3	^3Po	0.0	3.513E+00	3.462E+00
P XI, $N_{SS} = 290$					
K	Configuration	Level	J	E_{SS}(Ry)	E_{NIST}(Ry)
1	2*s*22*p*	^2Po	0.5	0.000E+00	0.000E+00
2	2*s*22*p*	^2Po	1.5	1.012E-01	8.838E-02
3	2*s*2*p*2	^4Pe	0.5	1.596E+00	1.615E+00
4	2*s*2*p*2	^4Pe	1.5	1.633E+00	1.646E+00
5	2*s*2*p*2	^4Pe	2.5	1.690E+00	1.692E+00
6	2*s*2*p*2	^2De	1.5	2.957E+00	2.887E+00
7	2*s*2*p*2	^2De	2.5	2.961E+00	2.888E+00
8	2*s*2*p*2	^2Se	0.5	3.747E+00	3.675E+00
9	2*s*2*p*2	^2Pe	0.5	4.011E+00	3.890E+00
10	2*s*2*p*2	^2Pe	1.5	4.070E+00	3.938E+00
P XII, $N_{SS} = 191$					
K	Configuration	Level	J	E_{SS}(Ry)	E_{NIST}(Ry)
1	1*s*22*s*2	^1Se	0.0	0.000E+00	0.000E+00
2	1*s*22*s*2*p*	^3P	2.0	1.7757E+00	1.784509
3	1*s*22*s*2*p*	$^3P0$	1.0	1.7104E+00	1.706532
4	1*s*22*s*2*p*	$^3P0$	0.0	1.6811E+00	1.670192
5	1*s*22*s*2*p*	$^1P0$	1.0	3.2746E+00	3.346967
6	1*s*22*p*2	^3Pe	0.0	4.410E+00	4.403E+00
7	1*s*22*p*2	^3Pe	1.0	4.454E+00	4.440E+00
8	1*s*22*p*2	^3Pe	2.0	4.524E+00	4.495E+00
9	1*s*22*p*2	^1De	2.0	5.001E+00	4.936E+00
10	1*s*22*p*2	^1Se	0.0	6.163E+00	6.057E+00
P XIII, $N_{SS} = 207$					
K	Configuration	Level	J	E_{SS}(Ry)	E_{NIST}(Ry)
1	1*s*22*s*	^2Se	0.5	0.000E+00	0.000E+00
2	1*s*22*p*	^2Po	0.5	1.893E+00	1.897E+00
3	1*s*22*p*	^2Po	1.5	2.016E+00	2.000E+00
4	1*s*23*s*	^2Se	0.5	2.542E+01	2.541E+01
5	1*s*23*p*	^2Po	0.5	2.594E+01	2.593E+01
6	1*s*23*p*	^2Po	1.5	2.597E+01	2.597E+01
7	1*s*23*d*	^2De	1.5	2.617E+01	2.616E+01
8	1*s*23*d*	^2De	2.5	2.618E+01	2.617E+01

Table 3. (*concluded*).

P XIII, $N_{SS} = 207$					
K	Configuration	Level	J	E_{SS}(Ry)	E_{NIST}(Ry)
9	1*s*24*s*	^2Se	0.5	3.408E+01	3.408E+01
10	1*s*24*p*	^2Po	0.5	3.430E+01	3.429E+01
P XIV, $N_{SS} = 120$					
K	Configuration	Level	J	E_{SS}(Ry)	E_{NIST}(Ry)
1	1*s*2	^1Se	0.0	0.000E+00	0.000E+00
2	1*s*2*s*	^3Se	1.0	1.563E+02	1.562E+02
3	1*s*2*p*	^3Po	0.0	1.573E+02	1.573E+02
4	1*s*2*p*	^3Po	1.0	1.574E+02	1.573E+02
5	1*s*2*s*	^1Se	0.0	1.574E+02	1.574E+02
6	1*s*2*p*	^3Po	2.0	1.575E+02	1.574E+02
7	1*s*2*p*	^1Po	1.0	1.583E+02	1.582E+02
8	1*s*3*s*	^3Se	1.0	1.848E+02	1.847E+02
9	1*s*3*p*	^3Po	0.0	1.851E+02	1.850E+02
10	1*s*3*s*	^1Se	0.0	1.851E+02	1.850E+02
P XV, N_{SS}=16					
K	Configuration	Level	J	E_{SS}(Ry)	E_{NIST}(Ry)
1	1*s*	^2Se	0.5	0.000E+00	0.000E+00
2	2*p*	^2Po	0.5	1.692E+02	1.692E+02
3	2*s*	^2Se	0.5	1.692E+02	1.692E+02
4	2*p*	^2Po	1.5	1.694E+02	1.693E+02
5	3*p*	^2Po	0.5	2.006E+02	2.006E+02
6	3*s*	^2Se	0.5	2.006E+02	2.006E+02
7	3*d*	^2De	1.5	2.007E+02	2.006E+02
8	3*p*	^2Po	1.5	2.007E+02	2.006E+02
9	3*d*	^2De	2.5	2.007E+02	2.006E+02
10	4*p*	^2Po	0.5	2.116E+02	2.115E+02

Note: N_{BPRM}, N_{SS} are the total number of energies obtained using BPRM approximation and SUPERSTRUCTURE (SS) program, respectively. BPRM, Breit–Pauli R-matrix.

Table 4. Comparison of the present A-values in s^{-1} for allowed E1 and forbidden E2, M1 transitions in P I– XV with other published values. Nt_{BPRM} and Nt_{SS} are the total number of transitions obtained from BPRM method and SS.

	P I: $Nt_{BPRM} = 32\,678$, $Nt_{SS} = 38\,565$		$A\ (s^{-1})$
Type	Transition	Present (BPRM, SS)	Others
E1	$3s^23p^3\left(^4S^o_{3/2}\right) \rightarrow 3s^23p^24s\left(^4P^o_{3/2}\right)$	2.017E+08,2.22E+08	[a] 2.17E+08, [b]2.043E+08
E1	$3s^23p^3\left(^4S^o_{3/2}\right) \rightarrow 3s^23p^24s\left(^4P^o_{3/2}\right)$	2.002E+08,2.26E+08	[a] 2.14E+08, [b]2.013E+08
E1	$3s^23p^3\left(^4S^o_{3/2}\right) \rightarrow 3s^23p^24s\left(^4P^o_{1/2}\right)$	1.99E+08,2.28E+08	[a] 2.13E+08, [b]2.013E+08
E1	$3s^23p^3\left(^4S^o_{3/2}\right) \rightarrow 3s3p^4\left(^4P_{1/2}\right)$	1.757E+06,9.27E+07	[c] 3.9E+07, [b]3.568E+05
E1	$3s^23p^3\left(^4S^o_{3/2}\right) \rightarrow 3s3p^4\left(^4P_{3/2}\right)$	2.105E+06,9.53E+07	[c] 4.0E+07, [b]4.332E+05
E1	$3s^23p^3\left(^4S^o_{3/2}\right) \rightarrow 3s3p^4\left(^4P_{5/2}\right)$	2.860E+06,9.99E+07	[c] 3.9E+07, [b]6.229E+05
E1	$3s^23p^3\left(^4S^o_{3/2}\right) \rightarrow 3s3p^24s\left(^2D_{5/2}\right)$	6.199E+04,1.71E+04	[d]4.4E+04
E1	$3s^23p^3\left(^4S^o_{3/2}\right) \rightarrow 3s^23p^24s\left(^2D_{3/2}\right)$	1.109E+04,3.05E+03	[c]8.20E+03
E1	$3s^23p^3\left(^4S^o_{3/2}\right) \rightarrow 3s^23p^24s\left(^2P_{3/2}\right)$	3.389E+05,2.16E+04	[c]2.60E+05
E1	$3s^23p^3\left(^4S^o_{3/2}\right) \rightarrow 3s^23p^24s\left(^2P_{1/2}\right)$	1.813E+05,9.61E+03	[c]1.50E+05
E1	$3s^23p^3\left(^2D^o_{3/2}\right) \rightarrow 3s^23p^24s\left(^2D_{5/2}\right)$	1.916E+07,2.21E+07	[c]2.32E+07,[b]1.789E+07
E1	$3s^23p^3\left(^2D^o_{3/2}\right) \rightarrow 3s^23p^24s\left(^2D_{3/2}\right)$	2.253E+08,2.84E+08	[c]2.54E+08,[b]2.174E+08
E1	$3s^23p^3\left(^2D^o_{5/2}\right) \rightarrow 3s^23p^24s\left(^2D_{5/2}\right)$	2.352E+08,2.93E+08	[c]2.64E+08

Table 4. (*continued*).

	P I: $Nt_{BPRM} = 32\,678$, $Nt_{SS} = 38\,565$		$A\ (s^{-1})$
Type	Transition	Present (BPRM, SS)	Others
E1	$3s^23p^3\left(^2D^o_{5/2}\right) \rightarrow 3s^23p^24s\left(^2D_{3/2}\right)$	2.154E+07,2.73E+07	[c]2.28E+07
M1	$3s^23p^3\left(^4S^o_{3/2}\right) \rightarrow 3s^23p^3\left(^2P^o_{3/2}\right)$	1.07E-02	[d]1.08E-01
M1	$3s^23p^3\left(^4S^o_{3/2}\right) \rightarrow 3s^23p^3\left(^2P^o_{1/2}\right)$	4.30E-03	[d]4.26E-02
E2	$3s^23p^3\left(^4S^o_{3/2}\right) \rightarrow 3s^23p^3\left(^2P^o_{3/2}\right)$	1.16E-07	[d]3.30E-07
E2	$3s^23p^3\left(^4S^o_{3/2}\right) \rightarrow 3s^23p^3\left(^2P^o_{1/2}\right)$	2.16E-07	[d]4.70E-06
E2	$3s^23p^3\left(^2D^o_{3/2}\right) \rightarrow 3s^23p^3\left(^2P^o_{1/2}\right)$	6.22E-02	[d]8.00E-02
M1	$3s^23p^3\left(^2D^o_{3/2}\right) \rightarrow 3s^23p^3\left(^2P^o_{1/2}\right)$	1.75E-03	[d]2.11E-02
E2	$3s^23p^3\left(^2D^o_{3/2}\right) \rightarrow 3s^23p^3\left(^2P^o_{3/2}\right)$	3.11E-02	[d]4.05E-02
M1	$3s^23p^3\left(^2D^o_{3/2}\right) \rightarrow 3s^23p^3\left(^2P^o_{3/2}\right)$	2.81E-03	[d]3.41E-02
E2	$3s^23p^3\left(^2D^o_{5/2}\right) \rightarrow 3s^23p^3\left(^2P^o_{3/2}\right)$	7.24E-02	[d]9.40E-02
M1	$3s^23p^3\left(^2D^o_{5/2}\right) \rightarrow 3s^23p^3\left(^2P^o_{3/2}\right)$	1.58E-03	[d]1.90E-02
NIST ([a][9], [b][12], [c][15], [d][10]			
	P II: $Nt_{BPRM} = 23\,255$, $Nt_{SS} = 35\,092$		$A\ (s^{-1})$
Type	Transition	Present(BPRM,SS)	Others
E1	$3s^23p^2\left(^3P_0\right) \rightarrow 3s3p^3\left(^3D^o_1\right)$	9.023E+06,8.38E+06	[a] 7.2E+06, [g]8.312E+06
E1	$3s^23p^2\left(^3P_1\right) \rightarrow 3s3p^3\left(^3D^o_1\right)$	6.205E+06,5.40E+06	[a] 5.4E+06, [g]4.905E+06
E1	$3s^23p^2\left(^3P_1\right) \rightarrow 3s3p^3\left(^3D^o_2\right)$	1.198E+07,1.13E+07	[a] 9.6E+06, [g]1.339E+07
E1	$3s^23p^2\left(^3P_1\right) \rightarrow 3s3p^3\left(^1D^o_2\right)$	2.416E+06,4.38E+05	[g]3.249E+06
E1	$3s^23p^2\left(^3P_2\right) \rightarrow 3s3p^3\left(^3D^o_1\right)$	3.529E+05,2.61E+05	[a] 3.5E+05, [g]1.789E+05
E1	$3s^23p^2\left(^3P_2\right) \rightarrow 3s3p^3\left(^3D^o_2\right)$	3.369E+06,2.76E+06	[a] 3.20E+06
E1	$3s^23p^2\left(^3P_0\right) \rightarrow 3s3p^3\left(^3P^o_1\right)$	1.297E+07,1.00E+08	[b] 5.0E+07, [g]2.853E+07
E1	$3s^23p^2\left(^3P_1\right) \rightarrow 3s3p^3\left(^3P^o_1\right)$	1.073E+07,7.65E+07	[b] 3.7E+07,[g]1.652E+07
E1	$3s^23p^2\left(^3P_1\right) \rightarrow 3s3p^3\left(^3P^o_0\right)$	3.932E+07,3.02E+08	[b] 1.5E+08, [g]5.674E+07
E1	$3s^23p4s\left(^1P^o_1\right) \rightarrow 3s^23p4p\left(^1S_0\right)1$	8.920E+07,5.88E+07	[c]1.60E+08
E1	$3s^23p4s\left(^3P^o_0\right) \rightarrow 3s^23p4p\left(^3S_1\right)$	2.719E+07,8.70E+05	[c]1.20E+07
E1	$3s^23p4s\left(^3P^o_1\right) \rightarrow 3s^23p4p\left(^3S_1\right)$	1.572E+07,1.01E+07	[c]3.50E+07
E1	$3s^23p4s\left(^3P^o_0\right) \rightarrow 3s^23p4p\left(^3P_1\right)$	2.719E+07,4.71E+07	[c]3.20E+07
E2	$3s^23p^2(^3P_0) \rightarrow 3s^23p^2(^3P_2)$	2.14E-09	[d]6.60E-09, [g]8.02E-09
M1	$3s^23p^2(^3P_0) \rightarrow 3s^23p^2(^3P_1)$	4.45E-05	[e]8.05E-05, [g]2.533E-04
M1	$3s^23p^2(^3P_1) \rightarrow 3s^23p^2(^1S_0)$	1.61E-01	[d]2.20E-01, [g]2.65E-01
E2	$3s^23p^2(^3P_2) \rightarrow 3s^23p^2(^1S_0)$	2.00E-03	[d]6.30E-03, [g]3.305E-03
E2	$3s^23p^2(^3P_1) \rightarrow 3s^23p^2(^3P_2)$	5.74E-10	[d]1.54E-09
M1	$3s^23p^2(^3P_1) \rightarrow 3s^23p^2(^3P_2)$	2.23E-04	[e]3.80E-04, [g]3.15E-04
[a]:[16], [b]:[15], [c]:[17], [d]:[10], [g]:[19]			
	P III: $Nt_{SS} = 35\,849$		$A\ (s^{-1})$
Type	Transition	Present(SS)	Others
E1	$3s^23p\left(^2P^o_{1/2}\right) \rightarrow 3s3p^2\left(^2D_{3/2}\right)$	6.270E+07	[a] 5.5E+07, [d]5.044E+07
E1	$3s^23p\left(^2P^o_{1/2}\right) \rightarrow 3s3p^2\left(^2S_{1/2}\right)$	1.14E+09	[d]8.164E+08
E1	$3s^23p\left(^2P^o_{1/2}\right) \rightarrow 3s3p^2\left(^2P_{1/2}\right)$	4.69E+09	[d]4.474E+09
E1	$3s^23p\left(^2P^o_{1/2}\right) \rightarrow 3s3p^2\left(^2P_{3/2}\right)$	1.29E+09	[d]1.186E+09
E1	$3s^23p\left(^2P^o_{1/2}\right) \rightarrow 3s^23d\left(^2D_{3/2}\right)$	7.05E+09	[d]6.520E+09
E1	$3s^23d\left(^2D_{3/2}\right) \rightarrow 3s^24p\left(^2P^o_{3/2}\right)$	2.40E+07	[b]1.0E+07
E1	$3s^24s\left(^2S_{1/2}\right) \rightarrow 3s^24p\left(^2P^o_{1/2}\right)$	1.78E+08	[b]1.40E+08
E1	$3s^24p\left(^2P^o_{1/2}\right) \rightarrow 3s^24d\left(^2D_{3/2}\right)$	4.57E+08	[b]3.90E+08
E1	$3s^24p\left(^2P^o_{3/2}\right) \rightarrow 3s^24d\left(^2D_{3/2}\right)$	9.06E+07	[b]7.70E+07
E1	$3s^24p\left(^2P^o_{3/2}\right) \rightarrow 3s^24d\left(^2D_{5/2}\right)$	5.43E+08	[b]4.60E+08
E1	$3s^23p\left(^2P^o_{1/2}\right) \rightarrow 3s3p^2\left(^4P_{1/2}\right)$	1.11E+04	[d]6.276E+03

Table 4. (*continued*).

	P III: $Nt_{SS} = 35\,849$		$A\ (s^{-1})$
Type	Transition	Present(SS)	Others
E1	$3s^2 3p\left(^2P^o_{1/2}\right) \rightarrow 3s3p^2\left(^4P_{3/2}\right)$	8.96E+01	[d]4.195E+01
M1	$3s^2 3p\left(^2P^o_{1/2}\right) \rightarrow 3s^2 3p\left(^2P^o_{3/2}\right)$	9.38E-04	[c]1.57E-03, [d]5.688E-03
[a][15], [b][17], [c][28], [d][27]			
	P IV: $Nt_{SS} = 6093$		$A\ (s^{-1})$
Type	Transition	Present(SS)	Others
E1	$3s^2\left(^1S_0\right) \rightarrow 3s3p\left(^1P^o_1\right)$	4.04E+09	[d] 3.94E+09
E1	$3s3p\left(^1P^o_1\right) \rightarrow 3p^2\left(^1D_2\right)$	8.73E+07	[d] 1.8E+08, 1.01E+08 [c]
E1	$3s3p\left(^3P^o_1\right) \rightarrow 3p^2\left(^3P_2\right)$	8.69E+08	[e] 7.70E+08
E1	$3s3p\left(^3P^o_0\right) \rightarrow 3p^2\left(^3P^o_1\right)$	1.15E+09	[e] 1.01E+09
E1	$3p^2\left(^1D_2\right) \rightarrow 3p3d\left(^1P^o_1\right)$	1.31E+09	[d] 4.10E+08
E1	$3p^2\left(^3P_0\right) \rightarrow 3p3d\left(^3D^o_1\right)$	3.64E+09	[e] 3.60E+09
E1	$3p^2\left(^3P_1\right) \rightarrow 3p3d\left(^3D^o_2\right)$	4.97E+09	[e] 4.80E+09
E1	$3s^2\left(^1S_0\right) \rightarrow 3s4p\left(^1P^o_1\right)$	5.42E+08	[d] 1.50E+09
M1	$3s3p\left(^3P^o_0\right) \rightarrow 3s3p\left(^1P^o_1\right)$	6.12E-02	[a]7.80E-2
M1	$3s3p\left(^3P^o_1\right) \rightarrow 3s3p\left(^1P^o_1\right)$	4.84E-02	[a]6.30E00
M1	$3s3p\left(^3P^o_1\right) \rightarrow 3s3p\left(^3P^o_2\right)$	7.60E-02	[a]9.20E-2
M1	$3s3p\left(^3P^o_1\right) \rightarrow 3s3p\left(^3P^o_2\right)$	1.11E-03	[a]1.39E-3
M1	$3s3p\left(^3P^o_0\right) \rightarrow 3s3p\left(^3P^o_1\right)$	1.77E-04	[a]2.12E-4
E2	$3s^2(^1S_0) \rightarrow 3p^2(^1D_2)$	2.69E+04	2.422E+04 [c]
[d][32], [e][33], [a][28], [c] [35]			
	P V: $Nt_{SS} = 17\,390$		$A\ (s^{-1})$
Type	Transition	Present(SS)	Others
E1	$2p^6 3s\left(^2S_{1/2}\right) \rightarrow 2p^6 3p\left(^2P^o_{1/2}\right)$	1.22E+09	[c] 1.16E+09, 1.219E+09 [b]
E1	$2p^6 3s\left(^2S_{1/2}\right) \rightarrow 2p^6 3p\left(^2P^o_{3/2}\right)$	1.26E+09	[c] 1.20E+09, 1.253E+09 [b]
E1	$2p^6 3p\left(^2P^o_{1/2}\right) \rightarrow 2p^6 3d\left(^2D_{3/2}\right)$	3.25E+09	[c] 3.10E+09, 4.088E+09 [a]
E1	$2p^6 3p\left(^2P^o_{1/2}\right) \rightarrow 2p^6 4s\left(^2S_{1/2}\right)$	2.48E+09	[d] 2.5E+09, 2.447E+09 [b]
E1	$2p^6 3p\left(^2P^o_{3/2}\right) \rightarrow 2p^6 4s\left(^2S_{1/2}\right)$	4.98E+09	[d] 4.9E+09, 4.913E+09 [b]
E1	$2p^6 3p\left(^2P^o_{3/2}\right) \rightarrow 2p^6 3d\left(^2D_{5/2}\right)$	3.84E+09	[c] 3.62E+09
E1	$2p^6 3p\left(^2P^o_{3/2}\right) \rightarrow 2p^6 3d\left(^2D_{3/2}\right)$	6.38E+08	[c] 6.0E+08
E1	$2p^6 3s\left(^2S_{1/2}\right) \rightarrow 2p^6 4p\left(^2P^o_{3/2}\right)$	1.53E+09	[d] 1.10E+09
E1	$2p^6 3s\left(^2S_{1/2}\right) \rightarrow 2p^6 4p\left(^2P^o_{1/2}\right)$	1.57E+09	[d] 1.10E+09
E1	$2p^6 3d\left(^2D_{3/2}\right) \rightarrow 2p^6 4f\left(^2F^o_{5/2}\right)$	8.70E+09	[d] 8.80E+09
E1	$2p^6 3d\left(^2D_{5/2}\right) \rightarrow 2p^6 4f\left(^2F^o_{7/2}\right)$	9.32E+09	[d] 9.10E+09
E1	$2p^6 3d\left(^2D_{5/2}\right) \rightarrow 2p^6 4f\left(^2F^o_{5/2}\right)$	6.21E+08	[d] 6.30E+08
[a][35], [b][39], [c][33], [d][17]			
	P VI: $Nt_{SS} = 16\,731$		$A\ (s^{-1})$
Type	Transition	Present(SS)	Others
E1	$2s^2 2p^6\left(^1S_0\right) \rightarrow 2s^2 2p^5 3s\left(^1P^o_1\right)$	6.11E+10	[a] 4.9E+10, [b]1.781E+11
E1	$2s^2 2p^5 3p\left(^3S_1\right) \rightarrow 2s^2 2p^5 3d\left(^3P^o_0\right)$	3.004E+09	[b]2.761E+09
E1	$2s^2 2p^6\left(^1S_0\right) \rightarrow 2s^2 2p^5 3d\left(^1P^o_1\right)$	5.525E+11	[a] 4.7E+11, [b]1.475E+12
E1	$2s^2 2p^5 3p(^3D_2) \rightarrow 2s^2 2p^5 3d(^3D_2)$	1.820E+08	[b]1.600E+09
E1	$2s^2 2p^5 3p(^3D_2) \rightarrow 2s^2 2p^5 3d(^3D_1)$	2.727E+08	[b]8.025E+08
E1	$2s^2 2p^6\left(^1S_0\right) \rightarrow 2s^2 2p^5 3s\left(^3P^o_1\right)$	1.42E+10	[a] 7.4E+09, [b]2.830E+10
E1	$2s^2 2p^6\left(^1S_0\right) \rightarrow 2s^2 2p^5 3d\left(^3P^o_1\right)$	1.20E+09	[a] 1.6E+09, [b]3.819E+09
E1	$2s^2 2p^6\left(^1S_0\right) \rightarrow 2s^2 2p^5 3d\left(^3D^o_1\right)$	3.07E+10	[a] 6.7E+10, [b]1.103E+11

Table 4. (*continued*).

	P VI: $Nt_{SS} = 16\,731$		$A\ (s^{-1})$
Type	Transition	Present(SS)	Others
E1	$2s^2 2p^5 3p\,(^3S_1) \rightarrow 2s^2 2p^5 3d\,(^3F^o_2)$	1.085E+06	[b]6.100E+06
E1	$2s^2 2p^5 3p(^3S_1) \rightarrow 2s^2 2p^5 3d(^1D_2)$	3.491E+07	[b]1.794E+07
[a] [40], [b] [41]			
	P VII: $Nt_{SS} = 93\,962$		$A\ (s^{-1})$
Type	Transition	Present(SS)	Others
E1	$2s^2 2p^5\,(^2P^o_{3/2}) \rightarrow 2s2p^6\,(^2S_{1/2})$	2.658E+10	[a] 2.9E+10, [c]2.557E+10
E1	$2s^2 2p^5\,(^2P^o_{3/2}) \rightarrow 2s^2 2p^4 3s\,(^2P_{3/2})$	1.133E+11	[c]1.114E+11
E1	$2s^2 2p^5\,(^2P^o_{3/2}) \rightarrow 2s^2 2p^4 3s\,(^4P_{5/2})$	3.069E+08	[c]1.797E+08
E1	$2s^2 2p^5\,(^2P^o_{3/2}) \rightarrow 2s^2 2p^4 3s\,(^4P_{3/2})$	4.775E+09	[c]2.840E+09
E1	$2s^2 2p^5\,(^2P^o_{3/2}) \rightarrow 2s^2 2p^4 3s\,(^4P_{1/2})$	1.956E+07	[c]7.583E+06
E1	$2s^2 2p^5\,(^2P^o_{3/2}) \rightarrow 2s^2 2p^4 3s\,(^2P_{1/2})$	4.900E+10	[c]4.762E+10
E1	$2s^2 2p^5\,(^2P^o_{3/2}) \rightarrow 2s^2 2p^4 3s\,(^2D_{5/2})$	5.204E+10	[c]5.163E+10
E1	$2s^2 2p^5\,(^2P^o_{3/2}) \rightarrow 2s^2 2p^4 3s\,(^2D_{3/2})$	3.666E+09	[c] 4.421E+09
E1	$2s^2 2p^5\,(^2P^o_{1/2}) \rightarrow 2s2p^6\,(^2S_{1/2})$	1.247E+10	[a] 1.4E+10, [c]1.215E+10
E1	$2s^2 2p^5\,(^2P^o_{1/2}) \rightarrow 2s^2 2p^4 3s\,(^4P_{3/2})$	3.547E+08	[c]2.312E+08
E1	$2s^2 2p^5\,(^2P^o_{1/2}) \rightarrow 2s^2 2p^4 3s\,(^2P_{3/2})$	1.652E+10	[c]1.721E+10
E1	$2s^2 2p^5\,(^2P^o_{1/2}) \rightarrow 2s^2 2p^4 3s\,(^2P_{1/2})$	5.587E+10	[c]8.410E+10
E1	$2s^2 2p^5\,(^2P^o_{1/2}) \rightarrow 2s^2 2p^4 3s\,(^2D_{3/2})$	4.944E+10	[c]4.745E+10
M1	$2s^2 2p^5\,(^2P^o_{3/2}) \rightarrow 2s^2 2p^5\,(^2P^o_{1/2})$	15.0	[a] 6.89
[a][43], [b][28] c*[44]			
	P VIII: $Nt_{SS} = 120\,624$		$A\ (s^{-1})$
Type	Transition	Present(SS)	Others
E1	$2s^2 2p^4\,(^3P_2) \rightarrow 2s2p^5\,(^3P^o_2)$	1.260E+10	[a]1.4E+10,[d]1.466E+10
E1	$2s^2 2p^4\,(^3P_2) \rightarrow 2s2p^5\,(^1P^o_1)$	3.929E+08	[d]3.386E+08
E1	$2s^2 2p^4\,(^3P^o_2) \rightarrow 2s2p^5\,(^3P^o_1)$	4.011E+09	[a]8.3E+09, [d]4.701E+09
E1	$2s^2 2p^4\,(^3P^o_1) \rightarrow 2s2p^5\,(^3P^o_1)$	4.206E+09	[a]4.9E+09, [d]4.886E+09
E1	$2s^2 2p^4\,(^3P^o_1) \rightarrow 2s2p^5\,(^3P^o_0)$	1.727E+10	[a]1.9E+10, [d]2.0E+10
E1	$2s2p^5\,(^1P^o_1) \rightarrow 2p^6\,(^1S_0)$	5.483E+10	[d]6.500E+10
E1	$2s2p^5\,(^3P^o_1) \rightarrow 2p^6\,(^1S_0)$	1.157E+08	[d]9.868E+07
E2	$2s^2 2p^4(^3P_2) \rightarrow 2s^2 2p^4(^1S_0)$	2.31E-01	[b]1.80E-01
M1	$2s^2 2p^4(^3P_2) \rightarrow 2s^2 2p^4(^1D_2)$	4.78E+01	[c]2.87E+01
E2	$2s^2 2p^4(^3P_2) \rightarrow 2s^2 2p^4(^1D_2)$	3.04E-02	[b, c]1.40E-02
E2	$2s^2 2p^4(^3P_2) \rightarrow 2s^2 2p^4(^3P_1)$	3.11E-05	[b, c]1.9E-05
M1	$2s^2 2p^4(^3P_2) \rightarrow 2s^2 2p^4(^3P_1)$	7.28	[c]4.28
[a][43], [b][46], [c][28], [d][45]			
	P IX: $Nt_{SS} = 159\,101$		$A\ (s^{-1})$
Type	Transition	Present(SS)	Others
E1	$2s^2 2p^3(^4S_{3/2}) \rightarrow 2s2p^4(^4P_{1/2})$	5.230E+09	[a] 5.8E+09, [c]5.764E+09
E1	$2s^2 2p^3\,(^4S^o_{3/2}) \rightarrow 2s2p^4\,(^4P_{3/2})$	5.071E+09	[a] 5.7E+09, [c]5.606E+09
E1	$2s^2 2p^3\,(^4S^o_{3/2}) \rightarrow 2s2p^4\,(^4P^o_{5/2})$	4.813E+09	[a] 5.4E+09, 5.355E+09
E1	$2s^2 2p^3(^2D_{3/2}) \rightarrow 2s2p^4(^2D_{3/2})$	1.160E+10	[a] 1.10E+10, [c]1.282E+10
E1	$2s^2 2p^3(^2D_{3/2}) \rightarrow 2s2p^4(^2D_{5/2})$	3.382E+08	[a] 8.4E+08, [c]3.945E+08
E1	$2s^2 2p^3\,(^2P^o_{1/2}) \rightarrow 2s2p^4\,(^4P_{3/2})$	1.659E+04	[c]1.390E+04
E1	$2s^2 2p^3\,(^2P^o_{3/2}) \rightarrow 2s2p^4\,(^4P^o_{3/2})$	3.369E+06	[c]2.821E+06
E1	$2s^2 2p^3\,(^2P^o_{3/2}) \rightarrow 2s2p^4\,(^4P^o_{5/2})$	1.702E+06	[c]1.566E+06
M1	$2s^2 2p^3\,(^4S^o_{3/2}) \rightarrow 2s^2 2p^3\,(^2P^o_{3/2})$	2.38E+02	[b] 1.27E+02
E2	$2s^2 2p^3\,(^4S^o_{3/2}) \rightarrow 2s^2 2p^3\,(^2P^o_{3/2})$	2.22E-03	[b] 3.0E-03

Table 4. (*continued*).

	P IX: $Nt_{SS} = 159\,101$		$A\ (s^{-1})$
Type	Transition	Present(SS)	Others
M1	$2s^2 2p^3\left(^4S^o_{3/2}\right) \rightarrow 2s^2 2p^3\left(^2D^o_{5/2}\right)$	1.41E-01	[b] 4.41E-02
E2	$2s^2 2p^3\left(^4S^o_{3/2}\right) \rightarrow 2s^2 2p^3\left(^2D^o_{5/2}\right)$	3.67E-02	[b] 1.40E-02
[a][43], [b][28], [c][45]			
	P X: $Nt_{SS} = 113\,791$		$A\ (s^{-1})$
Type	Transition	Present(SS)	Others
E1	$2s^2 2p^2\left(^3P^o_0\right) \rightarrow 2s2p^3\left(^3D_1\right)$	1.993E+09	[a]1.8E+09, [e]2.101E+09
E1	$2s^2 2p^2\left(^3P_2\right) \rightarrow 2s2p^3\left(^3D^o_3\right)$	2.726E+09	[a]3.1E+09, [e]2.982E+09
E1	$2s2p^3\left(^1P^o_1\right) \rightarrow 2p^4\left(^1S_0\right)$	3.254E+10	[e]3.566E+10
E1	$2s2p^3\left(^3P^o_2\right) \rightarrow 2p^4\left(^3P_1\right)$	3.130E+09	[e]3.105E+09
E1	$2s^2 2p^2\left(^3P_0\right) \rightarrow 2s2p^3\left(^3P^o_1\right)$	2.319E+09	[e]2.494E+09
E1	$2s^2 2p^2\left(^3P_0\right) \rightarrow 2s2p^3\left(^3S^o_1\right)$	4.995E+09	[a]5.0E+09, [e]4.967E+09
E1	$2s^2 2p^2\left(^3P_0\right) \rightarrow 2s2p^3\left(^1P^o_1\right)$	2.895E+06	[e]1.710E+05
E1	$2s^2 2p^2(^3P_1) \rightarrow 2s2p^3(^5S_2)$	1.557E+05	[e]1.040E+05
E1	$2s^2 2p^2\left(^3P_2\right) \rightarrow 2s2p^3\left(^5S^o_2\right)$	3.566E+05	[e]2.478E+05
E1	$2s^2 2p^2\left(^3P_1\right) \rightarrow 2s2p^3\left(^3D^o_1\right)$	1.008E+09	[a]1.3E+09, [e]1.131E+09
E1	$2s^2 2p^2\left(^3P_1\right) \rightarrow 2s2p^3\left(^3D^o_2\right)$	2.544E+09	[a]2.4E+09, [e]2.708E+09
M1	$2s^2 2p^2(^3P_0) \rightarrow 2s^2 p^2(^3P_1)$	1.64	[b, c, d] 6.98E-01
E2	$2s^2 2p^2(^3P_0) \rightarrow 2s^2 p^2(^1D_2)$	2.52E-03	[c] 9.20E-04
E2	$2s^2 2p^2(^3P_0) \rightarrow 2s^2 p^2(^3P_2)$	6.29E-05	[c] 1.75E-05
[e][45], [a][43], [b][46], [c] [48], [d][28]			
	P XI: $Nt_{SS} = 57\,130$		$A\ (s^{-1})$
Type	Transition	Present(SS)	Others
E1	$2s^2 2p\left(^2P^o_{1/2}\right) \rightarrow 2s2p^2\left(^2P^o_{1/2}\right)$	1.063E+10	[a] 1.30E+10,[d]1.071E+10
E1	$2s^2 2p\left(^2P^o_{1/2}\right) \rightarrow 2s2p^2\left(^2P_{3/2}\right)$	3.430E+09	[a] 3.4E+09, [d]3.368E+09
E1	$2s^2 2p\left(^2P^o_{1/2}\right) \rightarrow 2s2p^2\left(^2S_{1/2}\right)$	7.104E+09	[a] 3.8E+09, [d]6.611E+09
E1	$2s^2 2p\left(^2P^o_{1/2}\right) \rightarrow 2s2p^2\left(^4P^o_{1/2}\right)$	7.236E+05	[d]5.972E+05
E1	$2s^2 2p\left(^2P^o_{1/2}\right) \rightarrow 2s2p^2\left(^4P^o_{3/2}\right)$	1.706E+04	[d]1.311E+04
E1	$2s^2 2p\left(^2P^o_{1/2}\right) \rightarrow 2s2p^2\left(^2D_{3/2}\right)$	2.482E+09	[a] 2.30E+09, [d]2.544E+09
E1	$2s2p^2\left(^4P_{3/2} \rightarrow 2p^3\left(^2D^o_{3/2}\right)\right)$	1.020E+07	[d]8.368E+06
E1	$2s2p^2\left(^4P_{1/2}\right) \rightarrow 2p^3\left(^4S^o_{3/2}\right)$	3.424E+09	[a] 3.1E+09, [d]3.306E+09
E1	$2s2p^2\left(^4P_{3/2}\right) \rightarrow 2p^3\left(^4S^o_{3/2}\right)$	6.621E+09	[a] 6.3E+09, [d]6.422E+09
E1	$2s2p^2\left(^2P^o_{3/2}\right) \rightarrow 2p^3\left(^2P^o_{1/2}\right)$	1.643E+09	[d]1.744E+09
M1	$2s^2 2p\left(^2P^o_{1/2}\right) \rightarrow 2s^2 2p\left(^2P^o_{3/2}\right)$	1.228E+01	[b] 8.19, [c]8.16
M1	$2s2p^2(^2P_{1/2}) \rightarrow 2s2p^2(^2P_{3/2})$	2.301	[c]7.717 / [b]8.184
[d] [45], [a] [43][b] [28], [c] [17]			
	P XII: $Nt_{SS} = 20\,857$		$A\ (s^{-1})$
Type	Transition	Present(SS)	Others
E1	$2s^2\left(^1S_0\right) \rightarrow 2s2p\left(^1P^o_1\right)$	7.622E+09	[d] 7.0E+09, 7.770E+09 [b]
E1	$2s^2\left(^1S_0\right) \rightarrow 2s2p\left(^3P^o_1\right)$	8.023E+05	[c] 8.6E+05, 6.025E+05 [b]
E1	$2s^2\left(^1S_0\right) \rightarrow 2s3p\left(^1P^o_1\right)$	8.12E+11	1.10E+12 [e],
E1	$2s2p\left(^3P^o_1\right) \rightarrow 2p^2\left(^3P_2\right)$	1.584E+09	[d] 1.5E+09, 1.586E+09 [b]
E1	$2s2p\left(^3P^o_2\right) \rightarrow 2p^2\left(^3P^o_2\right)$	4.299E+09	[d] 4.3E+09, 4.379E+09 [b]
E1	$2s2p\left(^1P^o_1\right) \rightarrow 2p^2\left(^1D_2\right)$	1.221E+09	[d]1.30E+09, 1.289E+09 [b]
E1	$2s2p\left(^1P^o_1\right) \rightarrow 2p^2\left(^1S_0\right)$	1.154E+10	1.217E+10 [b]
M1	$2s2p\left(^3P^o_0\right) \rightarrow 2s2p\left(^1P^o_1\right)$	1.171E+02	[a] 7.7E+01

Table 4. (*concluded*).

	P XII: $Nt_{SS} = 20\,857$		$A\,(s^{-1})$
Type	Transition	Present(SS)	Others
M1	$2s2p\,(^3P^o_1) \rightarrow 2s2p\,(^1P^o_1)$	8.719E+01	[a] 1.94E+03
M1	$2s2p\,(^3P^o_0) \rightarrow 2s2p\,(^3P^o_1)$	1.139	[a] 5.9E-01,
[b][45], [a][28], [c][49], [d][43], [e] [50]			
	P XIII: $Nt_{SS} = 28\,110$		$A\,(s^{-1})$
Type	Transition	Present(SS)	Others
E1	$1s^22s\,(^2S_{1/2}) \rightarrow 1s2s2p\,(^1S)\,(^2P^o_{1/2})$	4.081E+13	4.089E+13 [a]
E1	$1s^22s\,(^2S_{1/2}) \rightarrow 1s^22p\,(^2P^o_{1/2})$	9.150E+08	9.26E+08 [d], 9.380E+08 [b]
E1	$1s^22s\,(^2S_{1/2}) \rightarrow 1s^22p\,(^2P^o_{3/2})$	1.108E+09	1.09E+09 [d], 1.101E+09 *b*
E1	$1s^22s\,(^2S_{1/2}) \rightarrow 1s^23p\,(^2P^o_{1/2})$	6.26E+11	6.15E+11 [c],
E1	$1s^22s\,(^2S_{1/2}) \rightarrow 1s^23p\,(^2P^o_{3/2})$	6.21E+11	6.19E+11 [c],
E1	$1s^22p\,(^2P^o_{1/2}) \rightarrow 1s^23s\,(^2S_{1/2})$	8.86E+10	8.77E+10 [c],
E1	$1s^22p\,(^2P^o_{3/2}) \rightarrow 1s^23s\,(^2S_{1/2})$	1.83E+11	1.730E+11 [c],
E1	$1s^22p\,(^2P^o_{1/2}) \rightarrow 1s^23d\,(^2D_{3/2})$	1.58E+12	1.60E+12 [c],
E1	$1s^22p\,(^2P^o_{3/2}) \rightarrow 1s^23d\,(^2D_{3/2})$	3.16E+11	3.16E+11 [c],
E1	$1s^23s\,(^2S_{1/2}) \rightarrow 1s^23p\,(^2P^o_{3/2})$	1.44E+08	1.06E+08 [c],
E1	$1s^23p\,(^2P^o_{1/2}) \rightarrow 1s^23d\,(^2D_{3/2})$	6.28E+06	7.05E+06 [c],
[a] [42], [b] [45][c] [17], [d] [43]			
	P XIV: $Nt_{SS} = 8389$		$A\,(s^{-1})$
Type	Transition	Present(SS)	Others
E1	$1s^2\,(^1S_0) \rightarrow 1s2p\,(^1P^o_1)$	5.108E+13	5.022E+13 [a],5.018E+13 [b],5.03E+13 [c]
E1	$1s^2\,(^1S_0) \rightarrow 1s2p\,(^3P^o_1)$	2.614E+11	3.101E+11 [a],3.38E+11 [d],3.026E+11 [b],3.11E+11 [c]
E1	$1s^2\,(^1S_0) \rightarrow 1s3p\,(^3P^o_1)$	7.832E+10	1.15E+11 [d]
E1	$1s2p\,(^3P^o_1) \rightarrow 1s2s\,(^1S_0)$	2.713E+02	2.23E+03 [c]
E1	$1s2s\,(^3S_0) \rightarrow 1s3p\,(^3P^o_1)$	8.377E+11	8.61E+11 [d]
E1	$1s2s\,(^3S_1) \rightarrow 1s2p\,(^3P^o_1)$	1.623E+08	1.84E+08 [c]
E1	$1s2s\,(^3S_1) \rightarrow 1s2p\,(^3P^o_0)$	1.447E+08	1.75E+08 [c]
E1	$1s2s\,(^1S_0) \rightarrow 1s2p\,(^1P^o_1)$	8.494E+07	7.47E+07 [c]
E1	$1s2s\,(^3S_1) \rightarrow 1s2p\,(^1P^o_1)$	5.361E+06	6.22E+06 [c]
E1	$1s2s\,(^3S_1) \rightarrow 1s2p\,(^3P^o_2)$	2.121E+08	2.31E+08 [c],2.06E+08 [e]
M1	$1s^2(^1S_0) \rightarrow 1s2s(^3S_1)$	6.879E+05	7.36E+05 [c]
M1	$1s2s(^3S_1) \rightarrow 1s2s(^1S_0)$	1.513	1.81 [c]
[a][54], [b][42], [c][55], [d][70], [e][71]			
	P XV: $Nt_{SS} = 149$		$A\,(s^{-1})$
Type	Transition	Present(SS)	Others
E1	$1s\,(^2S_{1/2}) \rightarrow 2p\,(^2P^o_{1/2})$	3.159E+13	[a]3.1778E+13
E1	$1s\,(^2S_{1/2}) \rightarrow 2p\,(^2P^o_{3/2})$	3.160E+13	[a]3.1645E+13
E1	$1s\,(^2S_{1/2}) \rightarrow 3p\,(^2P^o_{1/2})$	8.246E+12	[a]8.4557E+12
E1	$2s(^2S_{1/2}) \rightarrow 4d(^2D_{3/2})$	5.498E+07	$6.0454E+07$
Type	Transition	Present(SS)	Others
M1	$1s(^2S_{1/2}) \rightarrow 2s(^2S_{1/2})$	1.467E+06	[a]1.4578E+06
M1	$1s(^2S_{1/2}) \rightarrow 3s(^2S_{1/2})$	6.803E+05	[a]6.4707E+05
E2	$1s(^2S_{1/2}) \rightarrow 3d(^2D_{3/2})$	6.952E+09	[a]6.7420E+09
M1	$2p\,(^2P^o_{1/2}) \rightarrow 4p\,(^2P^o_{1/2})$	2.133E+02	$2.2613E+02$
[a][56]			

We compare the present A-values from BPRM method with the existing ones. Although general agreement, particularly with orders of magnitude, are found among various calculations, differences are also noted. One reason for discrepancy was noted from identification of levels. The mixed levels often have different leading percentages from different

Table 5. Comparison of present calculated radiative lifetimes τ (in 10^{-9} s) of levels of P ions with available experimental values using beam–foil (BF) and fluorescence detection (FD) techniques, storage ring (SR), Cyclotron (CR), and other theoretical values.

K	Configuration	Level	τ (ns) Present (BPRM)	Experiment	Method	Theory
			P I			
1	$3s^23p^24s$	$^2D_{5/2}$	3.45	3.6 ± 0.4 [a]	BF	3.58 [c]
2	$3s^23p^24s$	$^4P_{5/2}$	4.956	4.8 ± 0.5 [a]	BF	4.89 [c]
3	$3s^23p^24p$	$^4S^o_{3/2}$	33.11	36.9 ± 1.8 [b]	FD	27.75 [c]
4	$3s^23p^24p$	$^2D^o_{3/2}$	51.11	41.6 ± 14.8 [b]	FD	50.2 [c]
5	$3s^23p^24p$	$^4P^o_{3/2}$	39.46	38.9 ± 6.2 [b]	FD	34.9 [c]
6	$3s^23p^24p$	$^4D^o_{3/2}$	48.19,	48.1 ± 8.2 [b]	FD	44.03 [c]
7	$3s^23p^24p$	$^4D^o_{5/2}$	47.89	48.4 ± 5.5 [b]	FD	43.84 [c]
8	$3s^23p^24p$	$^4D^o_{7/2}$	45.47	48.3 ± 4.4 [b]	FD	43.80 [c]
[a][13], [b], [14], [c][12]						
			P II			
1	$3s3p^3$	$^3D^o_3$	58.96	45 ± 10 [b]	BF	93.8 [c]
2	$3s3p^3$	$^3P^o_1$	21.37	14 ± 0.8 [a]	BF	12.22 [c]
3	$3s3p^3$	$^3P^o_2$	25.63	14.6 ± 0.5 [a]	BF	12.98 [c]
				9.0 ± 0.5 [b]	BF	
[a][20], [b][13], [c][12]						
			P III			
1	$3s3p^2$	$^2P_{3/2}$	0.13	0.20 ± 0.05 [a]	BF	0.15 [b]
2	$3s3p^2$	$^2D_{5/2}$	13.16	14 ± 2.0 [a]	BF	15.2 [b]
3	$3p^3$	$^2D_{5/2}$	7.49	1.8 ± 0.4 [a]	BF	11.18 [b]
4	$3s^24p$	$^2P^o_{3/2}$	2.14	2.8 ± 0.2 [a]	BF	2.41 [b]
5	$3s^24f$	$^2F^o_{7/2}$	0.91	0.70 ± 0.15 [a]	BF	
6	$3s3p4s$	$^4P^o_{5/2}$	0.65	0.5 ± 0.2 [a]	BF	
[a][13], [b][12]						
			P IV			
1	$2p^63s3p$	$^1P^o_1$	0.241	0.22 ± 0.02 [a]	BF	0.27 [d]
2	$2p^63p^2$	$^3P_2$	0.289	0.32 ± 0.03 [a]	BF	0.32 [d]
3	$2p^63p^2$	$^1D_2$	10.8	8.2 ± 0.8 [a]	BF	9.88 [d]
4	$2p^63s3d$	$^3D_3$	0.193	0.36 ± 0.05 [a]	BF	0.21 [d]
5	$2p^63s4p$	$^3P^o_2$	1.12	1.23 ± 0.09 [c]	BF	1.15 [d]
6	$2p^63s4p$	$^3P^o_1$	1.08	1.22 ± 0.09 [c]	BF	1.14 [d]
7	$2p^63s4d$	$^3D_1$	1.66	1.75 ± 0.2 [c]	BF	1.44 [d]
8	$2p^63s4f$	$^3F^o_4$	0.176	0.4 ± 0.1 [a]	BF	0.17 [d]
9	$2p^63s5p$	$^3P^o_2$	1.15	2.5 ± 0.15 [c]	BF	
10	$2p^63s5p$	$^3P^o_1$	1.26	2.48 ± 0.15 [c]	BF	
11	$2p^63p3d$	$^1D_2$	0.239	0.5 ± 0.3 [a]	BF	0.27 [d]
12	$2p^63p4s$	$^3P^o_0$	0.207	0.27 ± 0.04 [b]	BF	
[a] [13], [b] [36], [c] [37], [d] [12]						
			P V			
1	$2p^63p$	$^2P^o_{3/2}$	0.794	0.70 ± 0.15 [a]	BF	0.78 [c]
2	$2p^63d$	$^2D_{5/2}$	0.261	0.38 ± 0.06 [b]	BF	0.26 [c]
3	$2p^64s$	$^2S_{1/2}$	0.134	0.32 ± 0.05 [b]	BF	0.13 [c]
4	$2p^64f$	$^2F^o_{7/2}$	0.107	0.17 ± 0.03 [b]	BF	0.11 [c]
5	$2p^65f$	$^2F^o_{7/2}$	0.198	0.38 ± 0.06 [b]	BF	0.19 [c]
6	$2p^65g$	$^2G_{9/2}$	0.375	1.56 ± 0.23 [b]	BF	
[a][13], [b][38], [c][12]						
			P VI			
1	$1s^22s^22p^53s$	$^1P^o_1$	0.0164	0.018 ± 0.002 [a]	BF	0.0169 [b]

Table 5. (*concluded*).

			P VI			
2	$1s^2 2s^2 2p^5 3s$	$^3P^o_1$	0.0704	0.105 ± 0.007 [a]	BF	0.106 [b]
[a] [72], [b] [41]						
			P VIII			
1	$1s^2 2s^2 2p^4$	$^1D_2$	1.70E07	2.86E07 ± 8.0E04 [a]	SR	2.45E07 [b]
[a] [47], [b] [45]						
			P IX			
1	$1s^2 2s^2 2p^3$	$^2P^o_{1/2}$	7.01E06	1.01E07 ± 1.2E05 [a]	BF	9.95E06 [b]
2	$1s^2 2s^2 2p^3$	$^2P^o_{3/2}$	2.90E06	4.2E06 ± 1.0E05 [a]	SR	4.22E06 [b]
[a] [47], [b] [45]						
			P X			
1	$1s^2 2s^2 2p^2$	$^1D_2$	1.21E + 07	1.77E07 ± 3.5E04 [a]	SR	1.549E07 [c]
2	$1s^2 2s 2p^3$	$^3S^o_1$	0.022	0.028 ± 0.004 [b]	BF	0.023 [d]
3	$1s^2 2s 2p^3$	$^3P^o_1$	0.132	0.17 ± 0.01 [b]	F	0.172 [d]
4	$1s^2 2s 2p^3$	$^3P^o_2$	0.136	0.6 ± 0.1 [b]	BF	0.176 [e]
5	$1s^2 2s 2p^3$	$^3D^o_1$	0.330	0.42 ± 0.02 [b]	BF	0.323 [d]
6	$1s^2 2p^4$	$^1D_2$	0.0714	0.082 ± 0.006 [b]	BF	0.07 [f]
7	$1s^2 2p^4$	$^3P_2$	0.0367	0.045 ± 0.005 [b]	BF	0.038 [f]
[a] [47], [b] [51], [c] [45], [d] [17], [e] [73], [f] [74]						
			P XI			
1	$1s^2 2s 2p^2$	$^2P_{1/2}$	0.04854	0.055 ± 0.006 [a]	BF	0.052 [b]
2	$1s^2 2s 2p^2$	$^2D_{3/2}$	0.3596	0.11 ± 0.03 [a]	F	0.392 [c]
				0.425 ± 0.03 [a]		
3	$1s^2 2p^3$	$^2P^o_{3/2}$	0.05982	0.073 ± 0.04 [a]	BF	0.074 [d]
4	$1s^2 2p^3$	$^4S^o_{3/2}$	0.0513	0.062 ± 0.06 [a]	BF	0.059 [c]
				0.32 ± 0.05 [a]		
[a] [51], [b] [17], [c] [75], [d] [76]						
			P XII			
1	$1s^2 2s 2p$	$^1P^o_1$	0.131	0.14 ± 0.01 [a]	BF	0.12 [b]
2	$1s^2 2p^2$	$^1S_0$	0.0869	0.089 ± 0.01 [a]	BF	0.095 [b]
3	$1s^2 2p^2$	$^3P_2$	0.17	0.18 ± 0.01 [a]	BF	0.169 [b]
4	$1s^2 2p^2$	$^1D_2$	0.7598	0.79 ± 0.05 [a]	BF	0.75 [b]
[a] [52], [b] [77]						
			P XIII			
1	$1s 2s 2p$	$^4P^o_{5/2}$	0.1622	1.2 ± 0.1 [a]	CR	1.3 [b]
[a] [53], [b] [78]						
			P XIV			
1	$1s 2p$	$^3P^o_0$	6.90	4.8 ± 0.4 [a]	BF	
2	$1s 2p$	$^3P^o_2$	2.87	3.6 ± 0.1 [b]	CT	3.5 [c]
[a] [?], [b] [53], [c] [12]						

Note: Complete tables of lifetimes of all excited levels will be available online.

methods toward an LS state and can cause unrealistic discrepancy by the different identifications. This appears to be one main reason for differences in agreement for P II A-values. Although A-values of E1 transitions from BPRM method are preferable, we compare A-values from SS also in the table for accuracy estimation of their A-values for the forbidden transitions. We compare the present A-values from SS for E2 and M1 transitions with available values, and the agreement is in general good, except for $3s^2 3p^2(^3P_1) - 3s^2 3p^2(^3P_2)(E2)$ given that these transitions are much more weaker than E1 transitions.

We have found lifetimes of three levels belonging to configuration $3s3p^3$ of P II, measured by two groups [13, 20] and theoretically computed values by one group [12]. We compare the present values with them in Table 5. The present lifetime for $^3D^o_3$, 59 ns is close to the upper limit of experimental value of 55 ns [13]. However, 94 ns predicted by Froese-Fischer et al. [12] is much higher than the present as well as the experimen-

Fig. 1. Complete spectrum of P I for strong lines using 32 678 E1 transitions. The lower panel (*a*) presents line strength continuing up to far infrared (IR) region of 1M (Å) and reveals dominance in the optical and IR regions. The upper panel (*b*) elaborates the line features up to 31 000 (Å). This region shows wavelength regions of dominance. However, the intensity is lower than that in the far IR region.

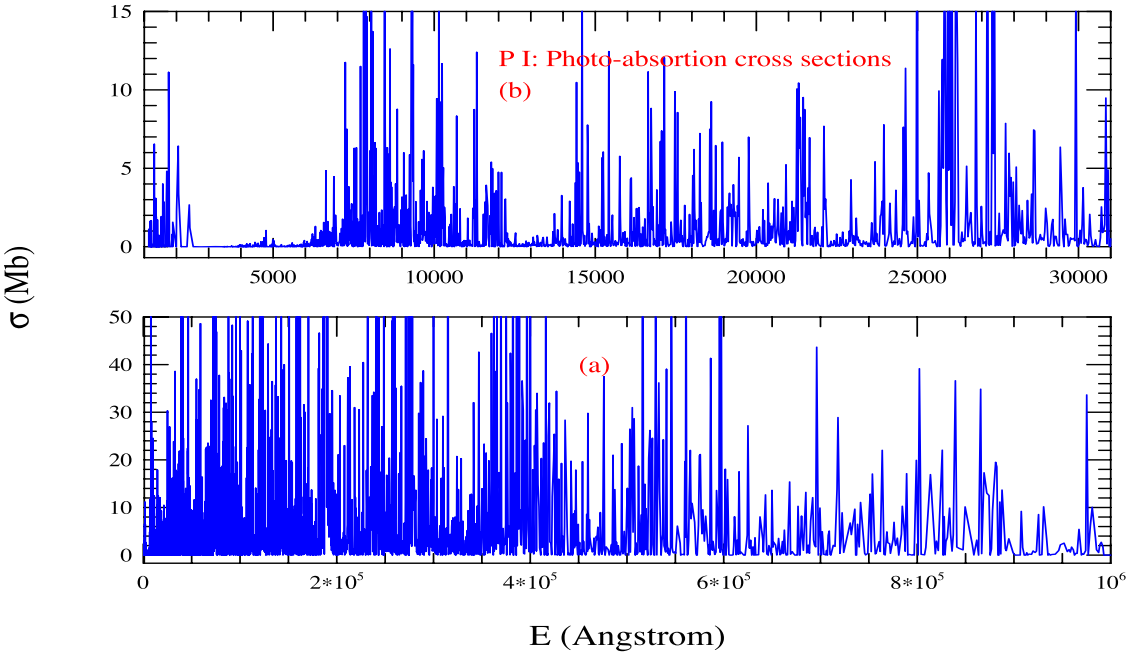

Fig. 2. The complete spectrum of P II for strong lines plotted with 23 255 E1 transitions. The lower panel (*a*) presents strengths up to far infrared (IR) region of 0.5M (Å) which indicate dominant regions up to 280 000 (Å). The upper panel (*b*) elaborates dominant regions in optical and IR wavelengths.

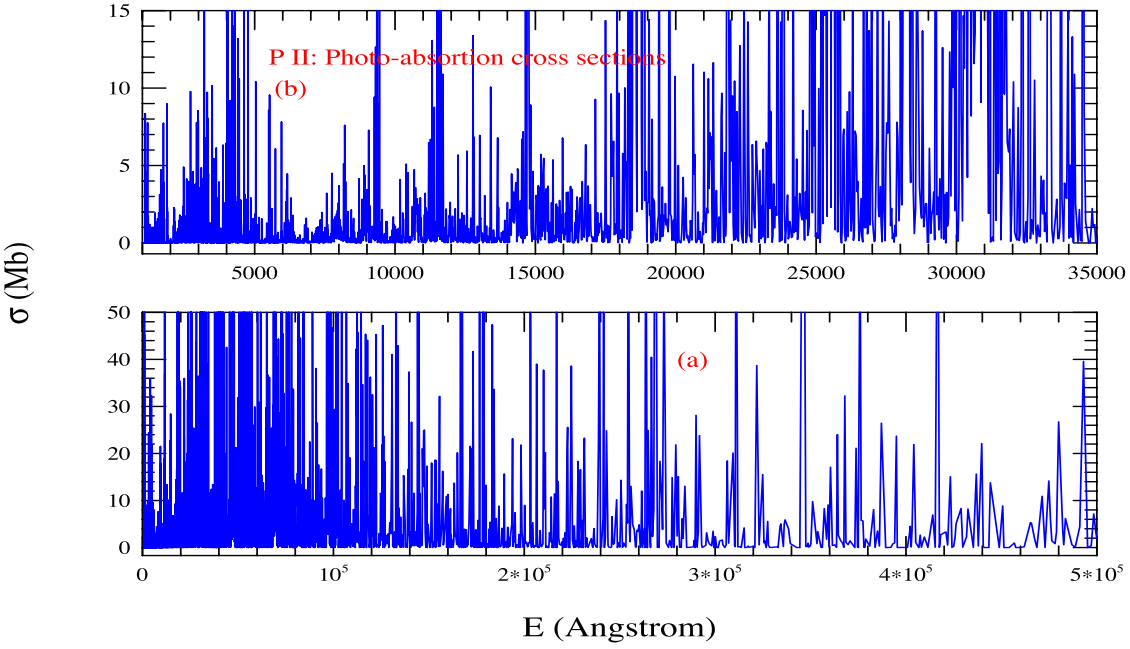

tal value. The other two lifetimes show that present lifetimes of $^3P^o_{1,2}$, about 21 and 25 ns, are higher than those of about 14 ns by Curtis et al. [13]. These again higher than the measured value of about 9 ns by Brown et al. [20] and theoretical prediction of about 12 ns by [12]. Some more study of lifetimes may confirm the accuracy of the values.

Features of photoabsorption spectrum of P II are presented in Fig. 2. Panel (*a*) shows the spectrum going up to 5×10^5 Å; wavelengths covering most of the strong lines of P II. The figure shows that the wavelength regions of line strengths, particularly up to far IR region of 3×10^5 Å; that dominate the spectrum and beyond which the density of strong lines

is reduced. The upper panel (*b*) elaborates the spectrum up to 35 000 (Å). a range covering for JWST. We note the density and strengths of lines dominate the region of 1700 to 35 000 (Å). This includes optical and IR regions. However, similar to P I, the strengths are lower than those in the far-IR regions.

4.3. P III

For the given set of configurations in Table 2, we have obtained 235 fine structure levels. Comparison in Table 3 shows differences of the calculated energies with the measured values are mainly in the third figure.

We report a total of 35 849 transition rates for Al-like phosphorus (P III) and 8441 of them are of type E1 transitions. A-values are compared with existing calculated values in Table 4. The present values comparable with Huang [27], Wiese et al. [17], and Fuhr et al. [15]. For the forbidden transition, $3s^2 3p\left(^2P^o_{1/2}\right) - 3s^2 3p\left(^2P^o_{3/2}\right)$, the present A-value 9.38E-04 s^{-1} is lower and that of Huang is 5.688E-03 s^{-1} which is higher than 1.57E-03 s^{-1} of Naqvi [28] which is rated as A in the NIST table.

For P III, lifetimes from 6 excited levels have been presented; two levels from the $3s3p^2$ configuration and one level from each of the configurations: $3p^3$, $3s^24p$, $3s^24f$, and $3s3p4s$. The present values compare very well with both experimental and the other theoretical values except for one even level $^2D_{5/2}$. The present value is higher than the experimental one. Predicted lifetime of Frose-Fischer is even higher than the present value.

Photoabsorption spectrum of P III is presented in Fig. 3. Unlike P I and P II, the spectrum does not extend to IR region. All strong lines appear in different regions of X-ray to ultraviolet wavelengths range. The reason for missing lines in the IR region could be not including transitions beyond than 5s.

4.4. P IV

From 18 configurations with orbitals going up to 5f, we have obtained 101 levels of P IV from SS. They agree very well with the measured values of Martin etl al [5], presented in Table 3.

We have obtained a total of 6093 allowed and forbidden transition out of which 1501 are E1 transitions. We compare the transition probabilities with those calculated by others [28, 32, 33, 35] and find very good agreement with them. The A-values of weak M1 transitions from the present work are also in very good agreement except one, $3s3p(3Po_1) - 3s3p(1Po_1)$, with those of Naqvi [28].

For P IV, lifetimes from 12 excited levels have been presented in Table 5. Our values compare very well with both experimental values of [13, 36, 37] except for one odd level ^4P and two even levels ^4S and ^2D. However they agree with all theoretical values by Frose-Fischer et al. [12].

Photoabsorption spectrum of P IV is presented in Fig. 4. As seen in the spectrum, spectral lines dominate the X-ray to ultraviolet wavelengths regions. However, P IV shows some dominant lines in the optical region going to near IR region.

4.5. P V

We have obtained 161 fine structure levels of P V from the given set of configurations going up to 5g given in Table 2. The energies have excellent agreement with the measured values of Martin et al. [5] in Table 3.

Transition rates for Na-like phosphorus (P V) have been calculated for 17 390 transitions of which 4309 are E1 transitions. The values are compared in Table 4 with those calculated by others [17, 33, 35, 39] with very good agreement.

For P V, lifetimes from six excited levels have been presented in Table 5. Our values compare very well with those predicted values of Frose-Fischer et al. [12]. Agreement is good with experimental values of [13], [38] except of a couple.

Photoabsorption spectrum of P V is presented in Fig. 5. The spectrum indicates dominant spectral lines in regions of soft X-ray to far ultraviolet wavelengths regions. The spectrum also indicates presence of some dominant lines in the optical region.

4.6. P VI

We have obtained 168 fine structure levels of P VI which are in less than 1% with most of the measured values of Martin et al. [5].

Transition rates for Ne-like phosphorus (P VI) have been calculated for 16 731 transition of which 3687 are E1 transitions. Examples are presented with comparison with those by Kaster et al. [40] (NIST included their values in the compiled table) and by Hibbert et al. [41] in Table 4. The present values compared much better with with those of Kastner et al. than of Hibbert et al [41].

For P VI, we compare the present lifetimes with lifetimes of two excited levels $3s^23p^23s\ (^1P^o_1, ^3P^o_1)$ measured by Trabert [72] and calculated by Hibbert et al. [41] in Table 5. Our value for $^1P^o_1$ compares very well with both experimental and theoretical ones. For the other level, our value is slightly lower than the measured range and that of Hibbert et al.

Photoabsorption spectrum of P VI is presented in Fig. 6. The regions of strong spectral lines extends from X-ray to IR (lower panel). The upper panel elaborates the region up to optical wavelengths.

4.7. P VII

We have obtained 386 fine structure levels for P VII which show large differences with the measured values of Martin et al. [5] as presented in Table 3.

Transition rates for F-like phosphorus (P VII) have been calculated for 93 962 transitions with 21 897 are of type E1. The values are compared with those calculated by Aggarwal [44], Cohen and Dalgarno [43] with very good agreement in Table 4. However, a single forbidden M1 transition by Naqvi [28] listed in the NIST has much lower value of 6.89 s^{-1} compared to the present value of 15 s^{-1}.

We have a large set of lifetimes for P VII, and have not found any published value to compare with.

Photoabsorption spectrum of P VII is presented in Fig. 7. The regions of strong spectral lines extends from X-ray to IR (lower panel). The upper panel elaborates the region up to optical wavelengths.

Fig. 3. The photoabsorption spectrum of P III plotted with 8441 E1 transitions demonstrates presence of strong lines in the X-ray to ultraviolet wavelength regions.

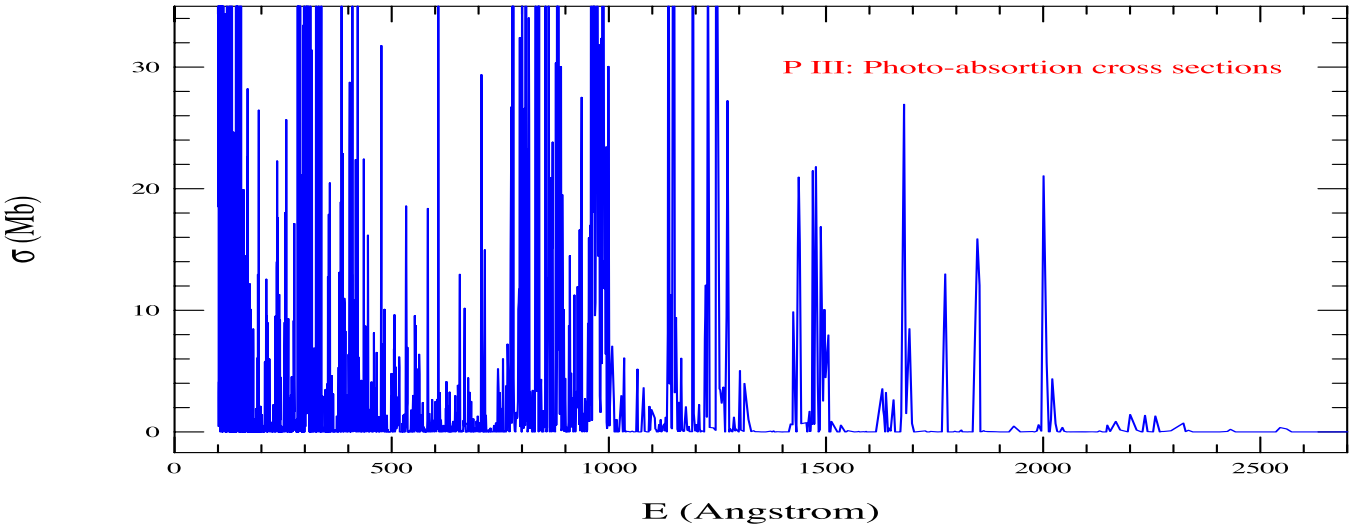

Fig. 4. The spectrum of P IV exhibiting strong lines in the X-ray to ultraviolet wavelength regions, and some isolated strong lines in the visible to near IR regions. A total of 1501 E1 transitions have been included in the spectrum.

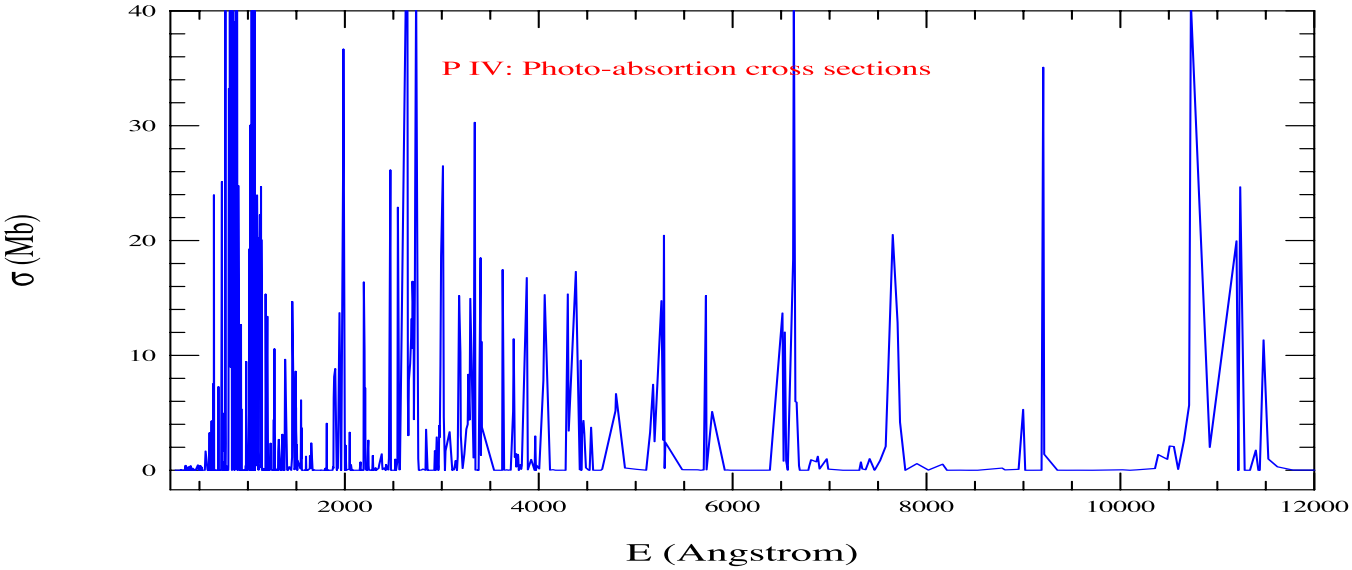

4.8. P VIII

We have obtained 653 fine structure levels of P VIII which are in less than 1 to a few percent differences with the measured values of Martin et al. [5] presented in Table 3.

Transition rates for O-like phosphorus (P VIII) have been calculated for 120 624 transitions with 59 219 are of type E1. The values are compared in Table 4 with those calculated by Cheng [45], Cohen and Dalgarno [43]. We find very good agreement between the present and reported values for the allowed transitions. For forbidden transitions, there are some differences with Naqvi [28] and Malville and Berger [46] but overall in agreement is acceptable as these transitions are very weak,

For P VIII, lifetime for 1 excited level from the ground configuration, $3s^2 3P^4(^1D_2)$ are presented. The lifetime is calculated from the forbidden transition. Our value 1.70E07 ns is comparable but lower than the measured lifetime 2:86E07 ns [47] and calculated value by Cheng [45].

Photoabsorption spectrum of P VIII is presented in Fig. 8. The regions of strong spectral lines extends from X-ray to IR (lower panel). The upper panel elaborates the region up to optical wavelengths.

4.9. P IX

We have obtained 498 fine structure levels of P IX. Comparison in Table 3 shows present values are in good agreement with those measured by Martin et al. [5].

We have calculated 159101 transition rates, which includes 37 203 E1 transitions, for N-like phosphorus, P IX. The values are compared in Table 4 with those calculated by Cheng [45],

Fig. 5. The spectrum of P V exhibiting strong lines in the regions of X-ray to far ultraviolet wavelength regions, and some isolated strong lines in the visible region. A total of 4309 E1 transition have been included in the spectrum.

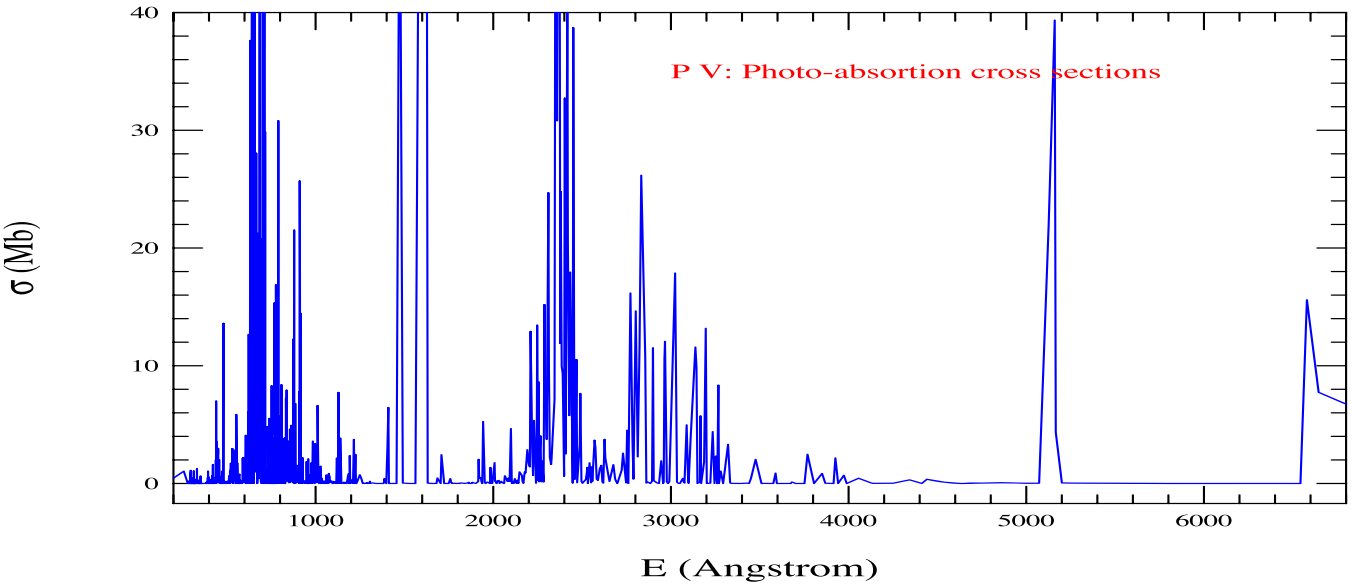

Fig. 6. The spectrum of P VI, created with 3687 E1 transitions is exhibiting strong lines in the regions of X-ray to infrared wavelengths in panel A. The upper panel elaborates the region of X-ray to optical.

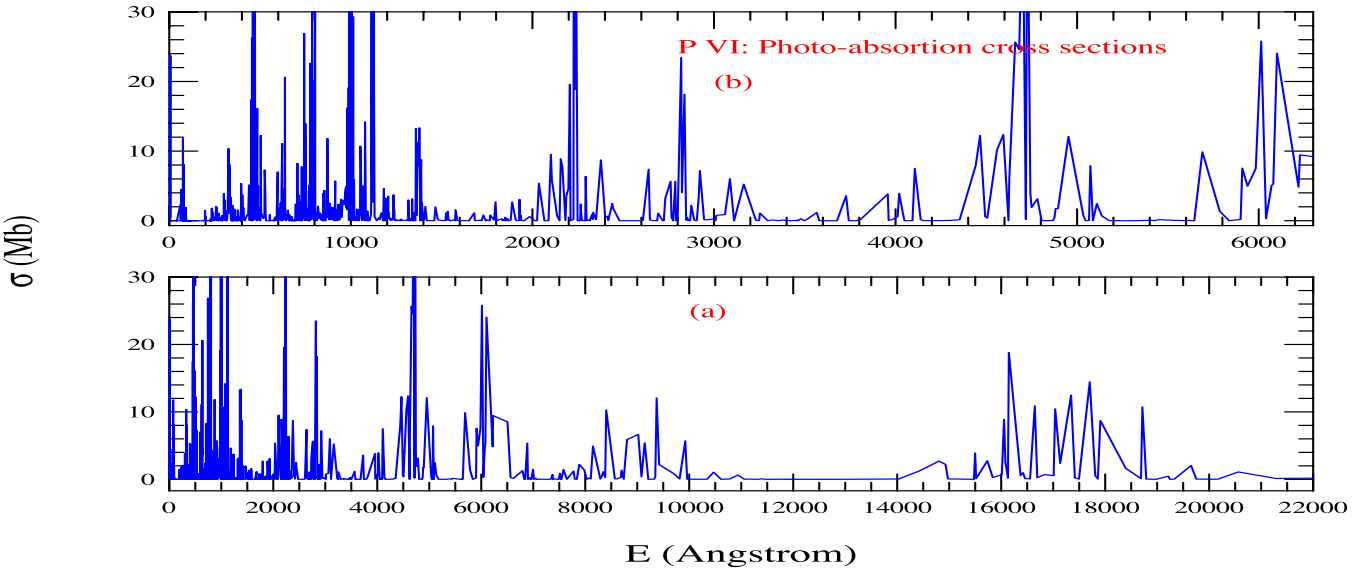

Cohen and Dalgarno [43], Naqvi [45]. Very good agreement is found among the present and those of Cheng, Cohen and Dalgarno for the allowed E1 transitions. Present A-values for forbidden transitions are comparable in order of magnitude with those by Naqvi [28].

For P IX, lifetimes from two excited levels $2s^2 2p^3(^2P^o 1/2, 3/2)$ from forbidden transitions, measured by Trabert [47], are presented in Table 5. The present lifetimes are comparable but somewhat lower than the published values.

Photoabsorption spectrum of P IX s presented in Fig. 9. The regions of strong spectral lines extends from X-ray to IR (lower panel). The upper panel elaborates the region up to optical wavelengths.

4.10. P X

We have obtained 430 fine structure levels of P X. Comparison in Table 3 shows good agreement with measured values.

We present a total of 113 971 transitions for P X of which 27 758 are of type E1. We present example transitions in Table 4 with comparison with Cheng [45], Cohen and Dalgarno [43], and Frose-Fischer [48] for the allowed transitions. Very good agreement are found among most of the transitions. Agreement of the present values varies with the forbidden transitions with those of Naqvi [28] and Malville and Berger [46].

For P X, lifetimes from seven excited levels are presented in Table 5. There has been more studies on this ion com-

Fig. 7. The spectrum of P VII, created with 21 897 E1 transitions, is exhibiting strong lines in the regions of X-ray to infrared wavelengths in panel (*a*). The upper panel (*b*) elaborates the region of X-ray to optical.

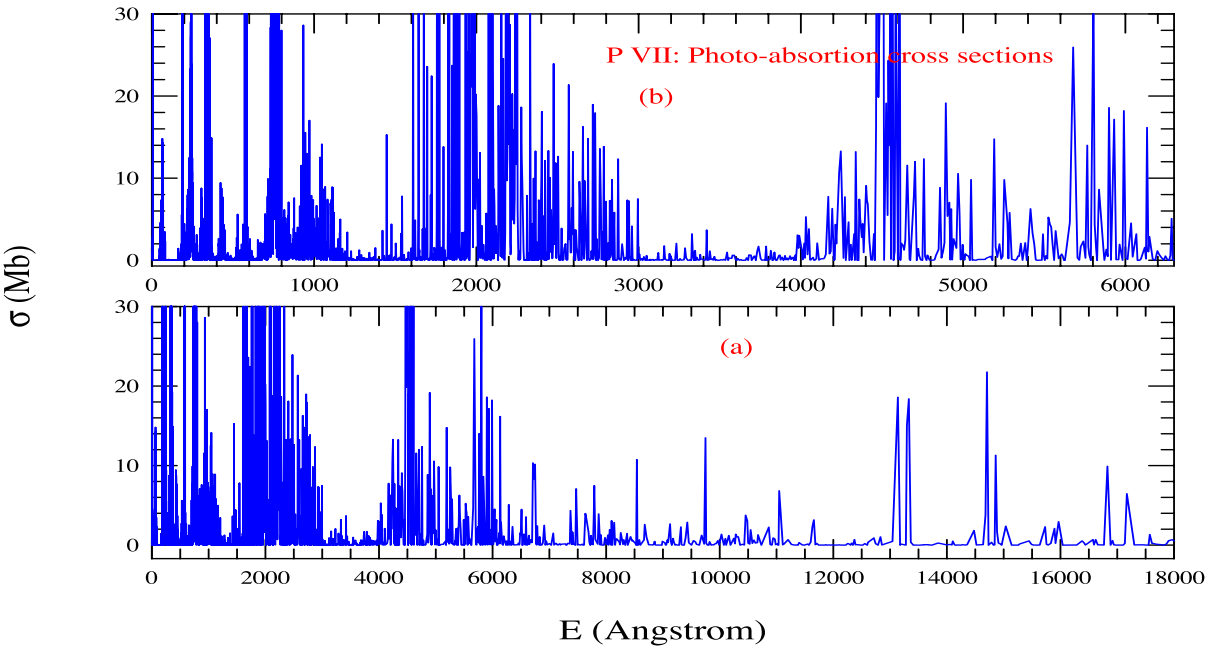

Fig. 8. The spectrum of P VIII, created with 59 219 E1 transitions. Exhibiting strong lines in the regions of X-ray to infrared wavelength. The upper panel elaborates the region of X-ray to optical.

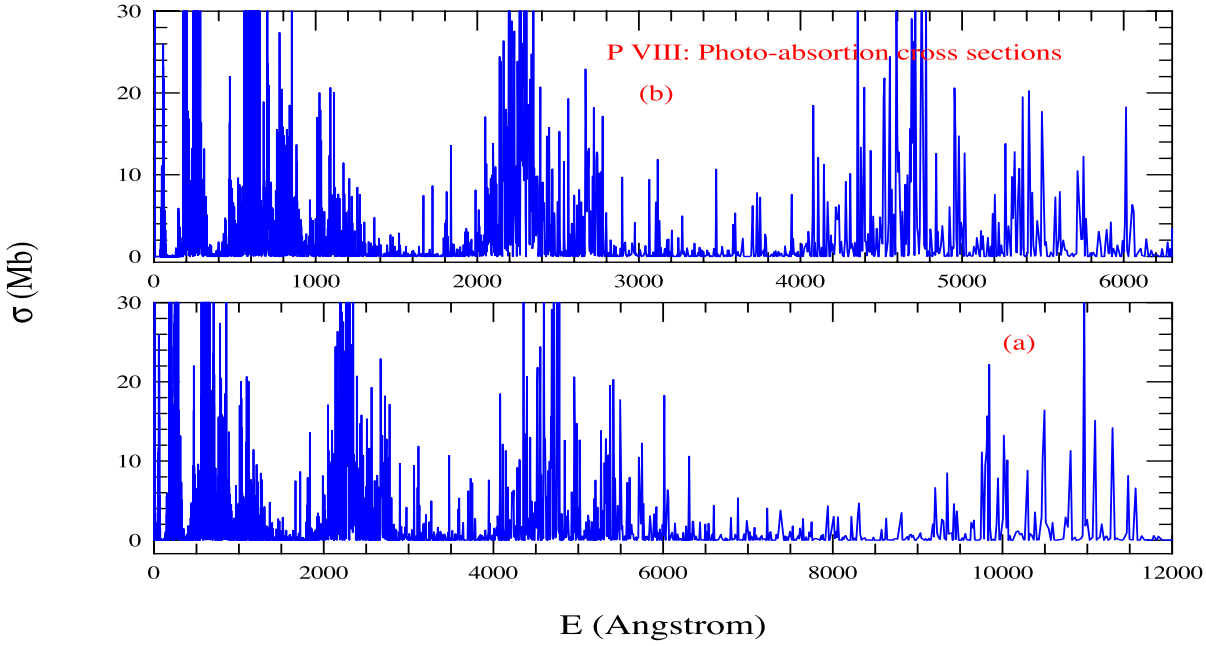

pared to other P ions. Our values for these levels compare very well with both experimental and theoretical ones [17, 45, 47, 51, 73, 74] except for one odd level $^3P^o_2$ for which experimental value is much larger than the theoretical predictions.

Photoabsorption spectrum of P-X is presented in Fig. 10. The regions of strong spectral lines extends from X-ray to optical but shows some lines in the IR (lower panel). The upper panel elaborates the region up to optical wavelengths.

4.11. P XI

We have obtained 290 fine structure levels of P XI which are in very good agreement with the measured values of Martin et al. [5] presented in Table 3.

With 290 levels, we have obtained 57130 transitions, including 14 446 transitions of type E1, for B-like phosphorus (P XI). We present sample A-values along with comparison with Cheng [45], Cohen and Dalgarno [43], Naqvi [28], and Wiese et al [17]. We find typical agreements,

Fig. 9. The spectrum of P IX, created with 37 203 E1 transitions, is exhibiting strong lines in the regions of X-ray to infrared wavelength in panel (*a*). The upper panels elaborates the region of X-ray to optical.

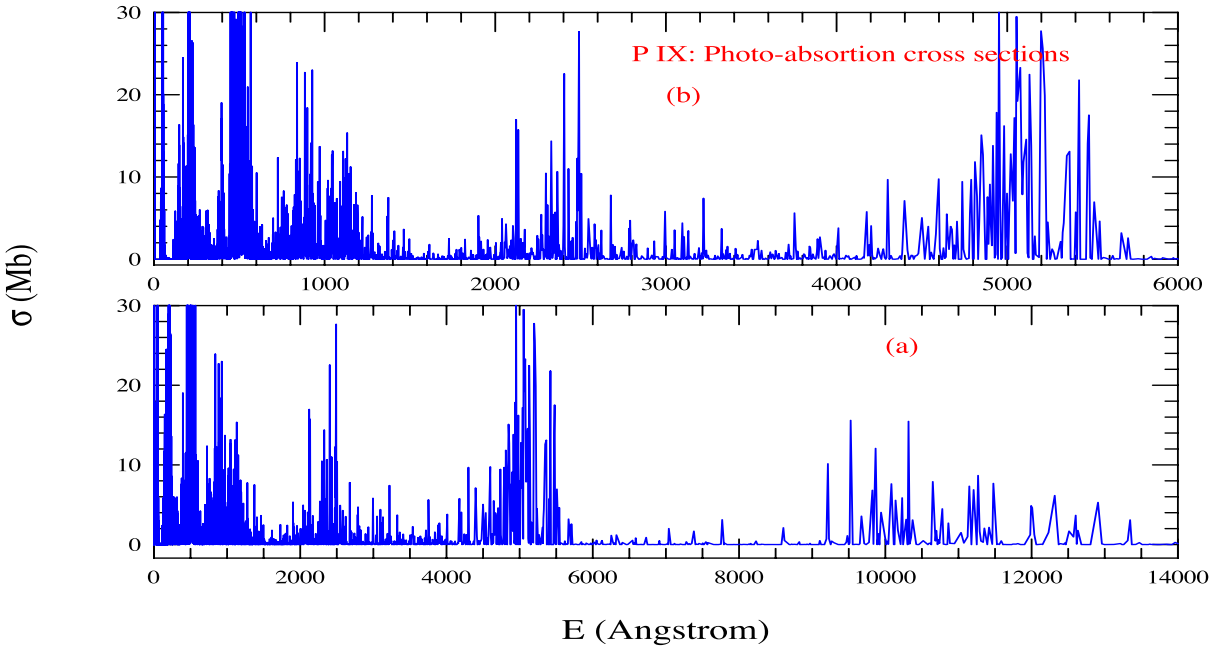

Fig. 10. The spectrum of P X, created with 27 758 E1 transitions, is exhibiting strong lines in the regions of X-ray to optical wavelengths in panels, but some in the infrared wavelength regions. The upper panels elaborates the region of X-ray to optical.

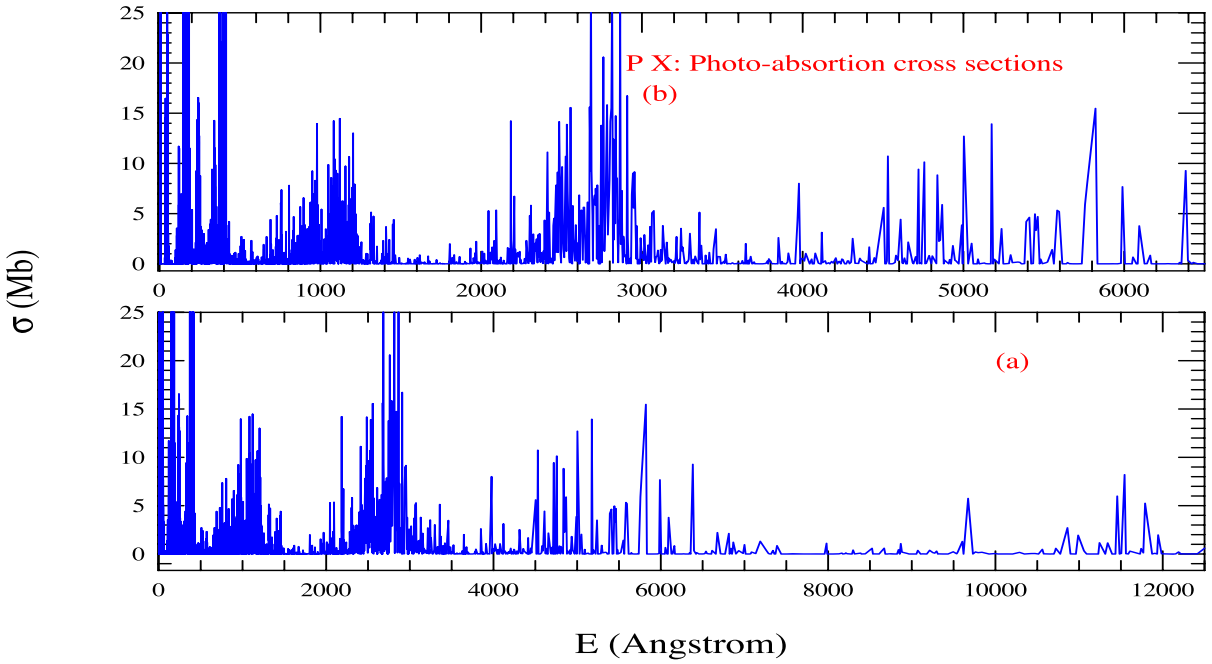

some transitions are very good agreement and some show differences.

For P XI, lifetimes of four excited levels are presented and compared in Table 5. General comparison of all lifetimes, theoretical and measured, show similar ranges of values although present values are slightly lower. Relatively large discrepancy between theory and experiment is noted for level $1s^2 2s 2p^2 (^2D_{3/2})$ where measured value is much lower than the predicted values.

Photoabsorption spectrum of P XI is presented in Fig. 11. The regions of strong spectral lines extends from X-ray to optical followed by sparse relatively weak lines.

Fig. 11. The spectrum of P XI, created with 14 446 E1 transitions, is exhibiting strong lines in the regions panel of X-ray to optical.

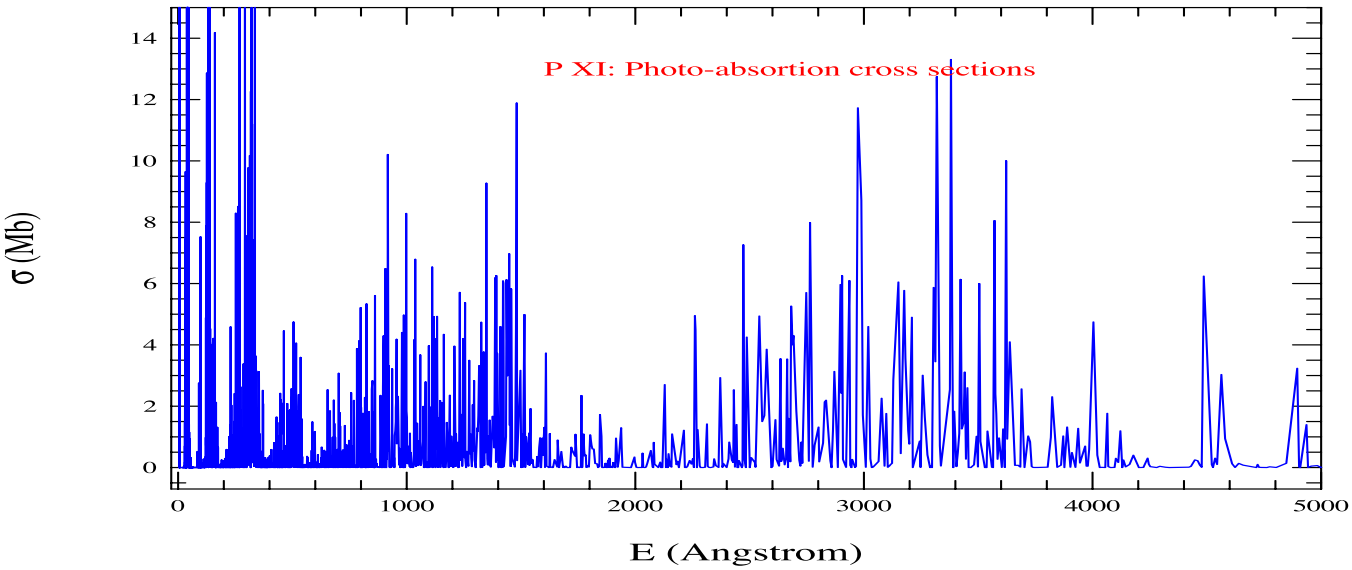

4.12. P XII

We have obtained 191 fine structure levels of P XII which are in about within 1% agreement with the measured values of Martin et al. [5] presented in Table 3.

Transition rates for Be-like phosphorus (P XII) have been calculated for 20 857 transitions including 4956 of type E1. Comparison with others have been made in Table 4 with Cheng [45], Naqvi [28], Garstrang and Shamey [49], Cohen and Dalgarno [43], and Naqvi and Victor [50]. The allowed transitions agree very well with each other. Like some other ions, present A-values for forbidden transitions have varying degrees of agreement with those of Naqvi.

For P XII, lifetimes from four excited levels are presented in Table 5. For this ion, very good agreement is found between the experimental and theoretical lifetimes for all levels.

Photoabsorption spectrum of P XII is presented in Fig. 12. The regions of strong spectral lines extends from X-ray to IR. Beyond 19 000 (Å), lines of moderate strength appear but sparsely.

4.13. P XIII

We have obtained 207 fine structure levels of P XIII which are in very good agreement with the measured values of Martin et al. [5] presented in Table 3.

We have calculated 28 110 transition rates, including 6841 for E1 transitions, for Li-like phosphorus (P XIII). Some of them are tabulated in Table 4 for comparison with those calculated by [17, 42, 43, 45] others [42, 45]. A very good agreement exists between the present and reported values.

A single measured lifetime for P XIII, $1s2s2p\left(tP^{o}_{5/2}\right.$, [53] is compared in Table 5. The present value 0.162 ns is comparable to the measured value 1.2 ± 0.1 ns and predicted value 1.3 ns [78]. Present value is slightly higher.

Photoabsorption spectrum of P XIII is presented in Fig. 13. The regions of visible spectral lines extends from X-ray to IR although becoming sparse after 13 000 (Å).

4.14. P XIV

We have obtained 120 fine structure levels of P XIII which are in very good agreement with the measured values of Martin et al. [5] presented in Table 3.

We have obtained transition rates for He-like phosphorus (P XIV) for 8389 transitions of which 2200 are of type E1. The present A-values are compared in Table 4 with those calculated by others [17, 42, 43, 45, 55] with very good agreement between the present and reported values for both allowed and forbidden transitions.

For P XIV, lifetimes of two excited levels presented and compared in Table 5. Present lifetimes are slightly higher and lower for the levels compared to the measured values and one predicted value.

Photoabsorption spectrum of P XIV is presented in Fig. 14. The regions of visible spectral lines extends from X-ray to IR although becoming sparse. The relative strengths of the lines are weaker than other P ions.

4.15. P XV

We have obtained 16 fine structure levels of P XV which are in less than 1 percent difference with the measured values of Martin et al [5] presented in Table 3.

We report transition rates for hydrogenic phosphorus (P XV) calculated for 149 transitions of which 42 are of type E1. The values are compared with those calculated by Popov [56] in Table 4. Very good agreement is found between the present and the available values for both allowed and forbidden transitions.

For P XV, only a limited number of lines appear in the X-ray region. They are presented in Fig. 15.

Fig. 12. The spectrum of P XII, created with 4956 E1 transitions, is exhibiting strong lines in the X-ray to infrared regions.

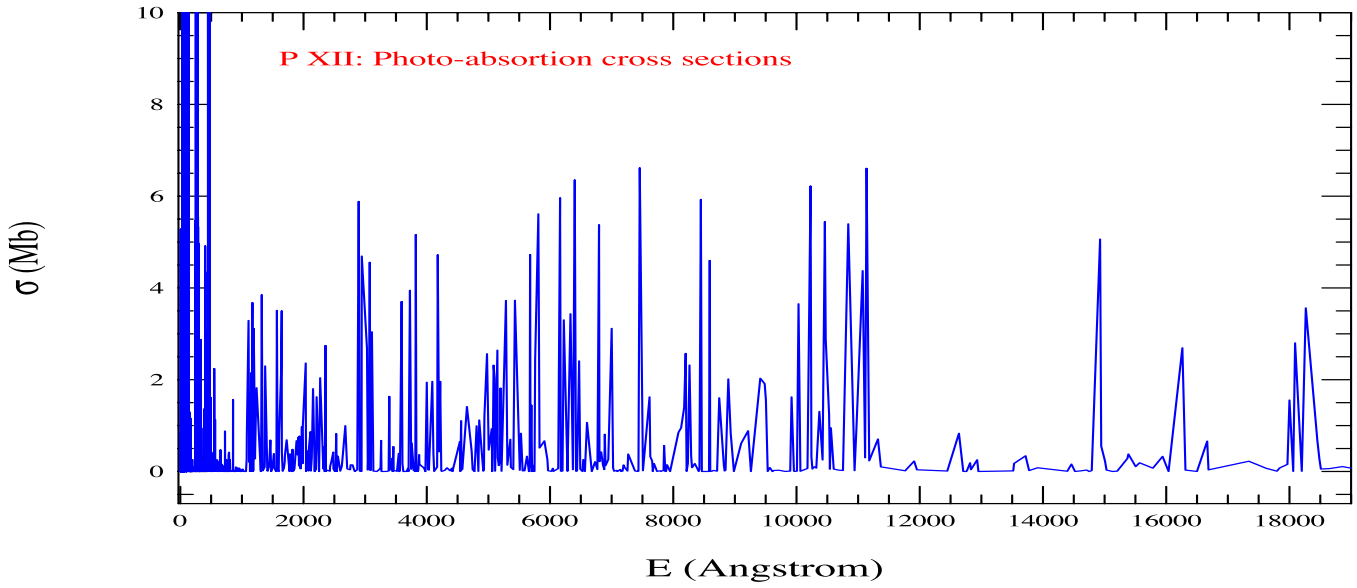

Fig. 13. The spectrum of P XIII, created with 6841 E1 transitions, is exhibiting visible lines in the regions of X-ray to infrared in panel (*a*). Spectral region up to 10 000 (Å) is elaborated in the upper panel.

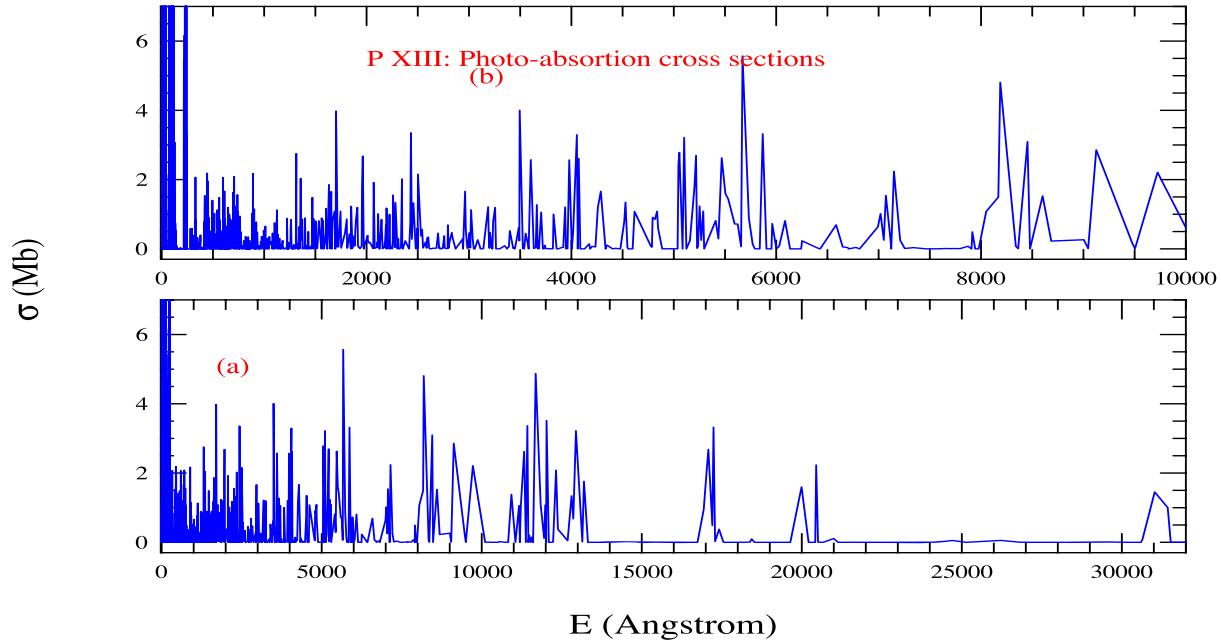

5. Conclusions

We conclude with the following points.

(i) We have carried out systematic study and present large sets of energy levels and transitions among them for all ionization stages of phosphorus, P I–P XV. The amount of atomic data obtained is much larger and complete than that available for most of phosphorus ions. The transitions are used to produce and study the spectral features of various ionization stages of phosphorus for the first time. The features can indicate presence of a P ion in an observed spectrum. The line strengths have been converted into photo-excitation cross sections to represent resonances in the synthetic spectrum of the ion. The high peak resonances indicate higher probability of excitation or ionization in the spectrum.

(ii) We present energies and transitions for P I and P II calculated using BPRM method for the first time for these ion and should be of high accuracy.

Fig. 14. The spectrum of P XIV, created with 2200 E1 transitions, is exhibiting visible lines in the regions of X-ray to infrared (IR). They become sparse in the IR region.

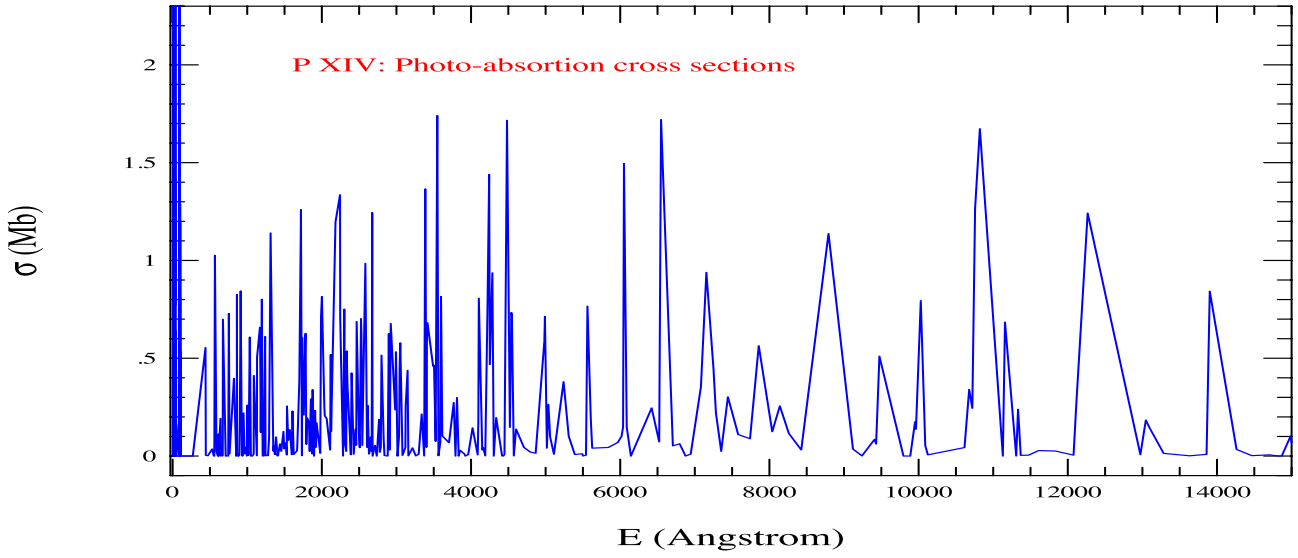

Fig. 15. The spectrum of P XV, created with 42 E1 transitions, is exhibiting a few strong lines in the X-ray region.

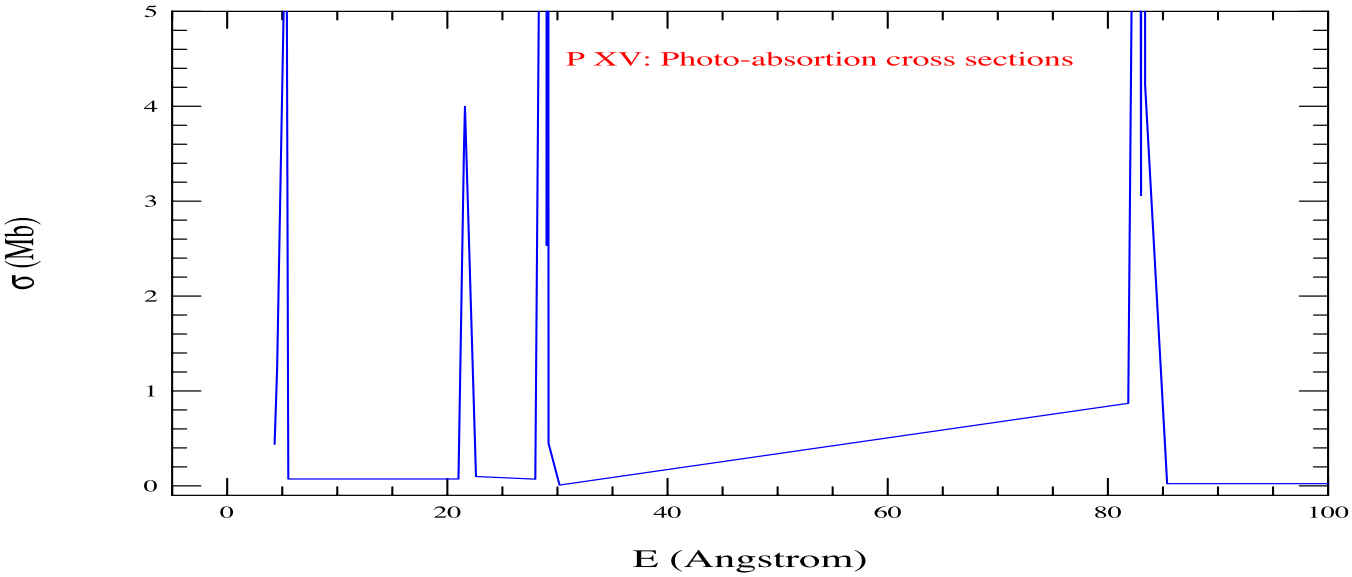

(iii) The present atomic data also include large sets of transition parameters for forbidden transitions of types E2, E3, M1, M2, applicable for various diagnostics.

(iv) Present level energies have been compared with measured energies compiled in NIST Atomic Database [8] with good agreement. Transition probabilities from the present work have been compared with theoretical values reported by other investigators and, good or general agreement is found for each P ion. Typically the same high precision calculation which includes large number of levels and transitions can agree well to some transition probabilities and not well with some other transitions. The reason is that some levels or transitions are optimized well and some are not in the calculations. In such a case, general agreement should be an indication of acceptable accuracy. The radiative lifetimes have been compared with experimental and theoretical values. We find very good agreement for some ions and general agreement for others.

(v) We attempted for the best optimization for SS to achieve high accuracy results for energies, transition probabilities, and radiative lifetimes for each ion. The accuracy is verified and confirmed with comparison with existing data. Comparisons indicate that the present atomic data for energies, transition probabilities, and radiative lifetimes, and spectroscopic guidance for detection of

phosphorus can be used for benchmarking until more accurate calculations of individual ions will be carried out using the R-matrix method or other fully relativistic approaches, which are expected to require significant amount of time.

(vi) The predicted spectra show considerable contributions in the IR regions by P I, P II and stretching strongly toward IR wavelengths by some other ions. Spectral features also indicate significant presence of some P-ions in the optical and UV regions. We have compiled atomic data and spectral features in a single article to study overall characteristics of the element.

Acknowledgments

The authors are thankful to the Ohio Supercomputer Center (OSC) for providing time slots to carry out all computations using its high performance computers.

Article information

History dates

Received: 6 October 2023
Accepted: 25 February 2024
Accepted manuscript online: 22 March 2024
Version of record online: 15 May 2024

Notes

This paper is part of a special issue entitled Bound States and Quantum Correlations — in honour of A. Ravi P. Rau

Copyright

Data availability

All atomic data will be available online at NORAD-Atomic-Data database at The Ohio State University: https://norad.astronomy.osu.edu/.

Author information

Author ORCIDs

Sultana N. Nahar https://orcid.org/0000-0002-8750-3836

Author notes

Present address for Bilal Shafique is Department of Physics, University of Azad Jammu & Kashmir, Muzaffarabad 13100, Pakistan.

Author contributions

Conceptualization: SNN
Data curation: SNN, BS
Formal analysis: SNN, BS
Funding acquisition: SNN, BS
Investigation: SNN, BS
Methodology: SNN
Project administration: SNN
Resources: SNN
Software: SNN
Supervision: SNN
Validation: SNN
Visualization: SNN, BS
Writing – original draft: SNN, BS
Writing – review & editing: SNN, BS

Competing interests

The authors declare there are no competing interests.

References

1. N.R. Hinkel, H.E. Hartnett, and P.A. Young. ApJ. Lett. **900**, L38 (2020). doi:10.3847/2041-8213/abb3cb.
2. P. Molaro, S.A. Levshakov, S. D'Odorico, and P. Bonifacio. Astrophys. J. **549**, 90 (2001). doi:10.1086/319072.
3. B.Y. Welsh, D.M. Sfeir, S. Sallmen S., and R. Lallement. Astron. Astrophys. **372**, 516 (2001). doi:10.1051/0004-6361:20010502.
4. B.C. Koo, Y.H. Lee, and D.S. Moon. Science, **342**(6164), 1346 (2013). doi:10.1126/science.1243823.
5. W.C. Martin, R. Zalubas, and A. Musgrove. J. Phys. Chem. Ref. Data, **14**, 751 (1985). doi:10.1063/1.555736.
6. V.A. Yerokhin and V.M. Shabaev. J. Phys. Chem. Ref. Data, **44**, 033103 (2015). doi:10.1063/1.4927487.
7. G.W. Erickson. J. Phys. Chem. Ref. Data, **6**, 831 (1977). doi:10.1063/1.555557.
8. National Institute of Standards and Technology (NIST). Gaithersburg, MD website: Kramida A, Ralchenko Yu, Reader J., and NIST ASD Team(2015), NIST Atomic Spectra Database (ver.5.3). Available from http://physics.nist.gov/PhysRefData/ASD/levels_form.html.
9. G.M. Lawrence. Astrophys. J. **148**, 261 (1967). doi:10.1086/149143.
10. S.J. Czyzak and T.K. Krueger. Mon. Not. R. Astron. Soc. **126**, 177 (1963). doi:10.1093/mnras/126.2.177.
11. O. Zatsarinny and C. Forse-Fischer. J. Phys. B At. Mol. Opt. Phys. **35**, 4669 (2002). doi:10.1088/0953-4075/35/22/309.
12. C. Forse-Fischer, G. Tachiev, and A. Irimia. Atom. Data Nucl. Data Tables, **92**, 607 (2006). doi:10.1016/j.adt.2006.03.001.
13. L.J. Curtis, I. Martinson, and R. Buchta. Phys. Scr. **3**, 197 (1971). doi:10.1088/0031-8949/3/5/001.
14. U. Berzinsh, S. Svanberg, and E. Biemont. Astron. Astrophys. **326**, 412 (1997).
15. J.R. Fuhr and W.L. Wiese. CRC Handbook of Chemistry and Physics, 79th Edition 10-88–10-146. *Edited by* D.R. Lide. CRC Press, Boca Raton, FL. 1998.
16. B.D. Savage and G.M. Lawrence. Astrophys. J. **146**, 940 (1966). doi:10.1086/148965.
17. W.L. Wiese, M.W. Smith, and B.M. Miles. Atomic Transition Probabilities. Vol. II, NSRDS-NBS 22, Washington.1969.
18. J.P. Desclaux. Comp. Phys. Comm. **9**, 31 (1975). doi:10.1016/0010-4655(75)90054-5.
19. K-N Huang. Atom. Data Nucl. Data Tables, **32**, 503 (1985). doi:10.1016/0092-640X(85)90022-1.
20. M.S. Brown, R.B. Alkhayat, R.E. Irving, N. Heidarian, J.B. Brown, S.R. Federman, S. Cheng, and L.J. Curtis. Astrophys. J. **868**, 42 (2018).
21. S.N. Nahar. New Ast. **50**, 19 (2017). doi:10.1016/j.newast.2016.07.003.
22. S.N. Nahar, E. M. Hernández, L. Hernández, et al. J. Quant. Spectrosc. Radiat. Transfer, **187**, 215 (2017). doi:10.1016/j.jqsrt.2016.09.013.
23. S.N. Nahar. Mon. Not. R. Astron. Soc. **469**, 3225 (2017). doi:10.1093/mnras/stx939.
24. S.N. Nahar and A.K. Pradhan. Phys. Rev. Lett. **68**, 1488 (1992). doi:10.1103/PhysRevLett.68.1488.
25. S.N. Nahar and A.K. Pradhan, Phys. Rev. A, **49**, 1816 (1994). doi:10.1103/PhysRevA.49.1816.
26. S.N. Nahar. Atoms, **8**,68 (2020). doi:10.3390/atoms8040068. Available from https://norad.astronomy.osu.edu/.
27. K.-N. Huang, Atom. Data Nucl. Data Tables, **34**, 1 (1986). doi:10.1016/0092-640X(86)90008-2.
28. A.M. Naqvi. Ph.D. thesis, Harvard University, 1951. p. 192.

29. L. Hernándeza, A.M. Covingtonb, E.M. Hernándeza, d, A. Antillóna, A. Morales-Moria, K. Chartkunchandb, A. Aguilarc, and G. Hinojosa. J. Quant. Spectrosc. Radiat. Transf. **159**, 80 (2015). doi:10.1016/j.jqsrt.2015.03.009.
30. M.T. Gning, J.K. Badiane, A. Diallo, M. Diouldé Ba, and I. Sakho. Nucl. Sci. **44**, 34 (2019). doi:10.11648/j.ns.20190404.11.
31. R. Naghma, S.N. Nahar, and A.K. Pradhan. MNRAS Lett. **479**, L60 (2018). doi:10.1093/mnrasl/sly095.
32. R.N. Zare. J. Chem. Phys. **47**, 3561 (1967). doi:10.1063/1.1712423.
33. R.J.S. Crossley and A. Dalgarno. Proc. R. Soc. Lond. Ser. A, **286**, 510 (1965).
34. C.D. Lin, C. Laughlin, and G.A. Victor, Astrophys. J, **220**, 734 (1978). doi:10.1086/155956.
35. M. Godefroid, C.E. Magnusson, P.O. Zetterberg, and I. Joelsson. Phys. Scr. **32**, 125 (1985). doi:10.1088/0031-8949/32/2/006.
36. R.B. Alkhayat. Ph.D. thesis, University of Toledo, USA. 2019.
37. P. Van Der Westhuizen, T.C. Kotze, and P.B. Kotze. J. Quant. Spectrosc. Radiat. Trans. **41**(5), 363 (1989). doi:10.1016/0022-4073(89)90066-6.
38. A.D. Maio. Ph.D. thesis, University of Arizona, USA. 1976.
39. W.R. Johnson, Z.W. Liu, and J. Sapirstein. Atom. Data Nucl. Data Tables, **64**, 279 (1996). doi:10.1006/adnd.1996.0024.
40. S.O. Kastner, K. Omidvar, and J.H. Underwood. Astrophys. J. **148**, 269 (1967). doi:10.1086/149144.
41. A. Hibbert, M.L. Dourneuf, and M. Mohan. Atom. Data Nucl. Data Tables, **53**, 23 (1993). doi:10.1006/adnd.1993.1002.
42. X.J. Zhu, B.L. Deng, C.Y. Zhang, S.P. Shi, and G. Jiang. Indian J. Phys. **90**, 2 (2016).
43. M. Cohen and A. Dalgarno. Proc. R. Soc. Lond. Ser. A, **280**, 258 (1964).
44. K.M. Aggarwal. Atom. Data Nucl. Data Tables, **125**, 226 (2019). doi:10.1016/j.adt.2018.03.001.
45. K.T. Cheng, Y.-K. Kim, and J.P. Desclaux. Atom. Data Nucl. Data Tables, **24**, 111 (1979). doi:10.1016/0092-640X(79)90006-8.
46. J. McKim Malville and R.A. Berger. Planet. Space. Sci. **13**, 1131 (1965). doi:10.1016/0032-0633(65)90143-1.
47. E. Träbert, E.M. Grieser, J. Hoffmann, C. Krantz, R. Repnow, and A. Wolf. Phys. Rev. A, **85**, 042508 (2012). doi:10.1103/PhysRevA.85.042508.
48. C. Froese. Astrophys J. **45**, 932 (1966). doi:10.1086/148833.
49. R.H. Garstang and L.J. Shamey. Astrophys. J. **148**, 665 (1967). doi:10.1086/149190.
50. A.M. Naqvi and G.A. Victor. TDR-63-3118. Harvard University, 1964. p. 627.
51. E. Träbert and P.H. Heckmann. Phys. Scr. **22**, 489 (1980). doi:10.1088/0031-8949/22/5/011.
52. E. Träbert and P.H. Heckmann. Phys. Scr. **21**, 35 (1980). doi:10.1088/0031-8949/21/1/006.
53. Ph. Deschepper, P. Lebrun, L. Palffy, and P. Pellegrin. Phys. Rev. A, **26**, 3 (1982).
54. G.W.F. Drake. Phys. Rev. A, **19**, 4 (1979).
55. C.D. Lin, W.R. Johnson, and A. Dalgarno. Phys. Rev. A, **15**, 1 (1977).
56. R.V. Popov and A.V. Maiorova. Opt. Spectr. **122**, 3 (2017).
57. The Opacity Project Team. The Opacity Project. Vol. **1**, 1995, Vol. 2, 1996, Institute of Physics Publishing.
58. D.G. Hummer, K.A. Berrington, W. Eissner, A.K. Pradhan, H.E. Saraph, and J.A. Tully. Astron. Astrophys. **279**, 298 (1993).
59. W. Eissner, M. Jones, and H. Nussbaumer. Comput. Phys. Commun. **8**, 270 (1974). doi:10.1016/0010-4655(74)90019-8.
60. S.N. Nahar, W. Eissner, G.X. Chen, and A.K. Pradhan. Astron. Astrophys. **408**, 789 (2003). doi:10.1051/0004-6361:20030945.
61. K.A. Berrington, P.G. Burke, K. Butler, M.J. Seaton, P.J. Storey, K.T. Taylor, and Y. Yu. J. Phys. B, **20**, 6379 (1987). doi:10.1088/0022-3700/20/23/027.
62. K.A. Berrington, W.B. Eissner, and P.H. Norrington. Comput. Phys. Commun. **92**, 290 (1995). doi:10.1016/0010-4655(95)00123-8.
63. A.K. Pradhan and S.N. Nahar. Atomic astrophysics and spectroscopy. Cambridge University press, New York. 2011. doi:10.1017/CBO9780511975349.
64. S.N. Nahar and A.K. Pradhan. Phys. Scr. **61**, 675 (2000). doi:10.1238/Physica.Regular.061a00675.
65. S N. Nahar. New Ast. **21**, 8 (2013). doi:10.1016/j.newast.2009.11.010.
66. S N. Nahar. Phys. Rev. A, **65**, 052702 (2002). doi:10.1103/PhysRevA.65.052702.
67. S.N. Nahar. In Proceedings of the 4th International Conference on MTPR-10, Modern Trends in Physics Research, Sharm El Sheikh, Egypt, December 12-16, 2010. *Edited by* L. El Nadi. World Scientific, 2013, pp. 275–285.
68. S.N. Nahar. Astron. Astrophys. **413**, 779 (2003).
69. S.N. Nahar. Phys. Scr. **55**, 200 (1997). doi:10.1088/0031-8949/55/2/012.
70. C. Laughlin. J. Phys. B: Atom. Molec. Phys. **11**, 13 (1978).
71. A. Dalgarno. NBS Special Publication No. 353. 1971. p. 47.
72. E. Träbert. Phys. Scr. **53**, 167 (1996). doi:10.1088/0031-8949/53/2/006.
73. C.A. Nicolaides and D.R. Beck. J. Phys. B, **6**, 535 (1973). doi:10.1088/0022-3700/6/3/022.
74. B.C. Fawcett. Atom. Data Nucl. Data Tables, **22**, 473 (1978). doi:10.1016/0092-640X(78)90020-7.
75. D.R. Flower and H. Nussbaumer. Astron. Astroph. **45**, 349. 79th ed. CRC Press, Boca Raton, FL, USA, 1975.
76. W. Dankwort and E. Trefftz. Astron. Astroph. **47**, 365 (1976).
77. B.C. Fawcett. Atom. Data Nucl. Data Tables, **22**, 473 (1978). doi:10.1016/0092-640X(78)90020-7.
78. K.-T. Cheng, C.P. Lin, and W.R. Johnson. Phys. Lett. **48A**, 437 (1974).